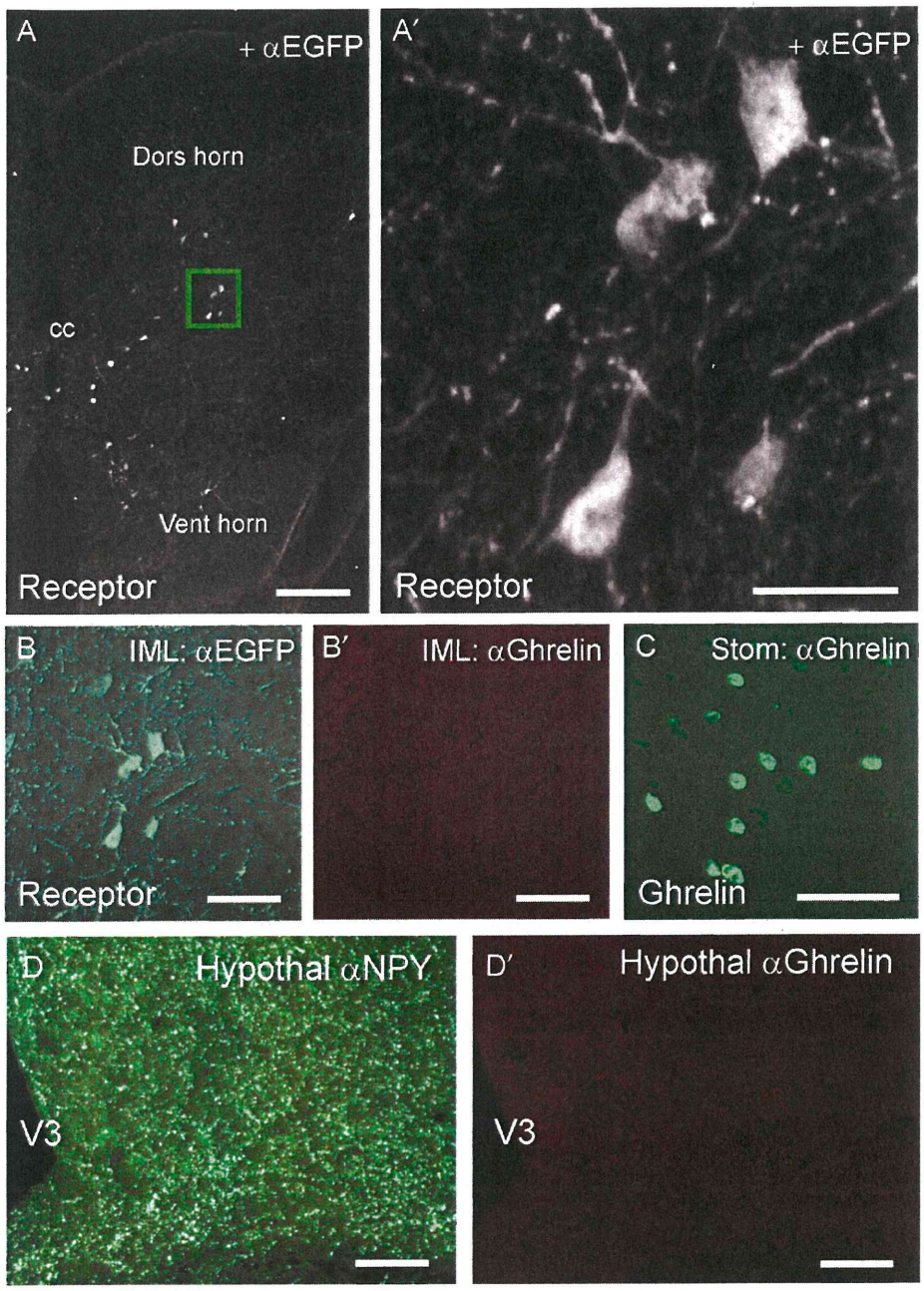

Fig. 4. Ghrelin receptor neurons and the localization of ghrelin peptide in a ghrelin receptor reporter mouse. (A) Locations of neurons that express the ghrelin receptor in a section through the lumbar spinal cord. An area of the intermediolateral cell nucleus (IML), containing ghrelin receptor expressing neurons, is outlined. The neurons have been localized using anti-EGFP. Landmarks labeled are the central canal (cc), the dorsal horn (Dors horn), and the ventral horn (Vent horn). (A′) Higher power view of the area that is marked in A. Receptor expression is seen in nerve cells and the initial parts of their dendrites, and in varicosities within the IML. (B, B′) Ghrelin receptor (B) and ghrelin (B′) immunoreactivity in the same field, using double staining. Note that no ghrelin is revealed in B′. (C) Localization of ghrelin in gastric endocrine cells of the reporter mouse using the identical immunohistochemical method of B, B′. Ghrelin immunoreactivity is strong in the endocrine cells. Results using antibody RY1601 are illustrated; the same observation was made with the other antibodies. (D, D′) Presence of NPY (D) and lack of ghrelin immunoreactivity (D′) in nerve terminals of the rat hypothalamus. The region illustrated is adjacent to the third ventricle (V3), an area that contains neurons with ghrelin receptors. Nerve terminals are revealed with anti-NPY, but none are revealed by anti-ghrelin (antibody GO1, 1:2000). Scale bars: (A), 250 μm; (A′), 25 μm; (B, B′ and C), 250 μm; (D, D′ and C), 100 μm. For interpretation of the references to color in this figure legend, the reader is referred to the Web version of this article.

say for ghrelin using ELISA showed that ghrelin-like material occurs in very low concentrations in extracts of CNS, compared to stomach, despite the fact that the gastric endocrine cells are a small proportion of the cells of the

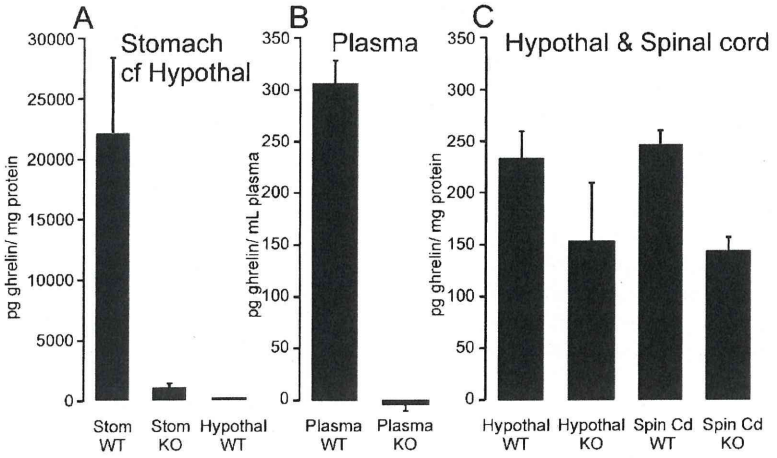

Fig. 5. Concentrations of immunoreactive ghrelin equivalents, determined by ELISA, in tissues and plasma of wild-type and ghrelin−/− mice. (A) Ghrelin-like material occurred in high concentrations in extracts of stomach of wild-type mice, but only in low amounts in the knockouts. Concentrations in the hypothalamus were about one hundredth of gastric concentrations. (B) Ghrelin-like material assayed in normal plasma was eliminated when the ghrelin gene was knocked out. (C) The small amounts of ghrelin-like material in the hypothalamus and spinal cord extracts were not significantly reduced by knock out of the ghrelin gene.

stomach wall. This parallels previous observations in rat (Hosoda et al., 2000) and sheep (Grouselle et al., 2008). In ghrelin knockout mice, the amount of ghrelin-like immunoreactivity in hypothalamic extracts was only partly reduced, suggesting that there may be a ghrelin-like substance in the CNS that is not a product of the ghrelin gene. If such a substance exists, it could have a low affinity for the ELISA assay, and thus it might be present in significant amount. Our result is consistent with the observations of Wortley et al. (2004), who found that ghrelin-like immunoreactivity of CNS neurons was unaffected by ablation of the ghrelin gene. It is possible that other products of the ghrelin gene are present in the wild-type animals. Ghrelin is derived from a longer 117 amino acid translation product, preproghrelin. This is predicted to provide several post-translation products, some of which contain ghrelin or ghrelin fragments (Seim et al., 2011). Moreover, alternative splicing may yield other species of preproghrelin, including partly frame-shifted products. In mouse hypothalamus, a transcript that retains intron 2 is the most abundant product of the ghrelin gene (Kineman et al., 2007). Thus, it is feasible that peptides are produced in the CNS that contain amino acid sequences in common with ghrelin, but that are not authentic ghrelin and that may or may not be acylated. It is also feasible that some anti-ghrelin antibodies react with such related peptides, which may explain some results that have been reported. Variations in published work include differences in places of localization of immunoreactivity and differences in cellular localization, for example different abilities to reveal nerve cells and nerve terminals, as we have summarized in the Introduction. At least some of the ghrelin-mimicking substance in mice is probably not a product of the ghrelin gene because, as elaborated in the Introduction, ghrelin reporter mice do not reveal expression in the CNS, whereas signal was observed in gastric endocrine cells (Wortley et al., 2004; Kageyama et al., 2008; Sakata et al., 2009). Although it might be considered that expression of transgenes is incomplete in the reporter mice, the results with the different reporter constructs all show lack of ghrelin, as do the present immunohistochemical studies. It is possible that authentic 28 amino-acid acylated ghrelin may be produced in some conditions of changed environment, physiological state, or behavior. Relevant to this consideration is the observation that ghrelin mRNA expression fluctuates with a circadian or ultradian rhythm and that the gene contains CLOCK-responsive E-box elements (Turek et al., 2005; Fick et al., 2010). The 24-h variation in ghrelin mRNA is abolished, and absolute levels are substantially reduced in *Clock* mutant mice (Turek et al., 2005). It is feasible that there are also circadian or ultradian influences on the products of ghrelin gene transcripts.

While this study and others suggest that ghrelin is not expressed in significant amounts in neurons in the CNS of rats or mice, the peptide may be present in other species. In particular, an immunohistochemical study of human brain revealed strong labeling of nerve fibers in hypothalamic nuclei, while no reaction was detected in neuronal cell bodies (Menyhért et al., 2006). The antibodies used in that study were raised against the unacylated form of ghrelin and reveal a 13 kDa proghrelin in Western blots (Cowley et al., 2003).

Although agonists of ghrelin receptors have effects within the forebrain, brain stem, and spinal cord, it is only in the forebrain that current data provides indications of roles of endogenous ghrelin on central neurons in addition to its established role in the stimulation of appetite. Peripherally administered ghrelin accesses a number of forebrain regions, including the hippocampus (Diano et al., 2006). Ghrelin enhances learning and memory and increases numbers of synapses per dendritic area in the hippocampus (Diano et al., 2006). Other central effects of increased circulating ghrelin, in physiologically relevant amounts, are anxiolytic and antidepressant actions (Lutter et al., 2008),

and increased expression of food-reward behavior (Perello et al., 2010; Chuang et al., 2011). Chuang et al. (2011) found that hedonic eating behavior induced by peripherally administered ghrelin was lost if ghrelin receptor expression was deleted and was restored when receptor expression was rescued selectively in catecholamine neurons. These data indicate that peripheral ghrelin accesses catecholamine neurons of the ventral tegmental area.

In the spinal cord, ghrelin receptor agonists or direct intrathecal administration of ghrelin activates autonomic preganglionic neurons that raise blood pressure, and increase colo-rectal motility and contractility of the bladder, but peripherally administered ghrelin is not effective (Shimizu et al., 2006; Ferens et al., 2010a,b; Hirayama et al., 2010). In the present work, we have shown that ghrelin-containing nerve endings do not impinge on the autonomic preganglionic neurons. The presence of functional ghrelin receptors on neurons, not innervated by ghrelin-containing synapses, that are in places that are not accessible to circulating or peripherally administered ghrelin suggests the presence of a natural, but unknown, receptor ligand in nerve terminals. In addition, the ghrelin receptor is constitutively active (Holst and Schwartz, 2004), and it is possible that modification of this constitutive activity, perhaps through an endogenous inverse agonist, has a controlling role for autonomic pathways. Thus, there is a need to look for effects of antagonists or inverse agonists on specific functions in order to determine roles for ghrelin receptors in regions of the CNS such as the spinal cord.

CONCLUSIONS

We conclude that there is little or no authentic ghrelin in the CNS of rats and mice housed under laboratory conditions. Ghrelin-like immunoreactivity that has been reported in these species is likely to be due to detection of precursors or substances that have sufficient similarity to ghrelin to cross-react with the antibodies. Neurons that express the ghrelin receptor are not innervated by nerve terminals that contain detectable ghrelin. Thus, the natural endogenous ligand for these receptors is unlikely to be ghrelin.

Acknowledgments—This work was supported by a grant from the National Health and Medical Research Council of Australia (grant number 1005811). We thank James Brock for helpful discussion of the project and the manuscript. Microscope facilities were provided by the Australian Phenomics Network Histopathology and Organ Pathology Node.

REFERENCES

Andrews ZB, Erion D, Beiler R, Liu ZW, Abizaid A, Zigman J, Elsworth JD, Savitt JM, DiMarchi R, Tschoep M, Roth RH, Gao XB, Horvath TL (2009) Ghrelin promotes and protects nigrostriatal dopamine function via a UCP2-dependent mitochondrial mechanism. J Neurosci 29:14057–14065.

Andrews ZB, Liu ZW, Walllingford N, Erion DM, Borok E, Friedman JM, Tschöp MH, Shanabrough M, Cline G, Shulman GI, Coppola A, Gao XB, Horvath TL, Diano S (2008) UCP2 mediates ghrelin's action on NPY/AgRP neurons by lowering free radicals. Nature 454:846–852.

Boyer PA, Trembleau A, Leviel V, Arluison M (1994) Effects of intranigral injections of colchicine on the expression of some neuropeptides in the rat forebrain: an immunohistochemical and in situ hybridization study. Brain Res Bull 33:541–560.

Canpolat S, Aydin M, Yasar A, Colakoglu N, Yilmaz B, Kelestimur H (2006) Effects of pinealectomy and exogenous melatonin on immunohistochemical ghrelin staining of arcuate nucleus and serum ghrelin leves in the rat. Neurosci Lett 410:132–136.

Chuang JC, Perello M, Sakata I, Osborne-Lawrence S, Savitt JM, Lutter M, Zigman JM (2011) Ghrelin mediates stress-induced food-reward behavior in mice. J Clin Invest 121:2684–2692.

Cowley MA, Smith RG, Diano S, Tschöp M, Pronchuk N, Grove KL, Strasburger CJ, Bidlingmaier M, Esterman M, Heiman ML, Garcia-Segura LM, Nillni EA, Mendez P, Low MJ, Sotonyi P, Friedman JM, Liu H, Pinto S, Colmers WF, Cone RD, Horvath TL (2003) The distribution and mechanism of action of ghrelin in the CNS demonstrates a novel hypothalamic circuit regulating energy homeostasis. Neuron 37:649–661.

Date Y, Murakami N, Toshinai K, Matsukura S, Niijima A, Matsuo H, Kangawa K, Nakazato M (2002) The role of the gastric afferent vagal nerve in ghrelin-induced feeding and growth hormone secretion in rats. Gastroenterology 123:1120–1128.

Diano S, Farr SA, Benoit SC, McNay EC, da Silva I, Horvath B, Gaskin FS, Nonaka N, Jaeger LB, Banks WA, Morley JE, Pinto S, Sherwin RS, Xu L, Yamada KA, Sleeman MW, Tschöp MH, Horvath TL (2006) Ghrelin controls hippocampal spine synapse density and memory performance. Nat Neurosci 9:381–388.

Ekblad E, Mulder H, Sundler F (1996) Vasoactive intestinal peptide expression in enteric neurons is upregulated by both colchicine and axotomy. Regul Pept 63:113–121.

Faulconbridge LF, Cummings DE, Kaplan JM, Grill HJ (2003) Hyperphagic effects of brainstem ghrelin administration. Diabetes 52:2260–2265.

Ferens DM, Yin L, Bron R, Hunne B, Ohashi-Doi K, Sanger GJ, Witherington J, Shimizu Y, Furness JB (2010a) Functional and in situ hybridisation evidence that preganglionic sympathetic vasoconstrictor neurons express ghrelin receptors. Neuroscience 166:671–679.

Ferens DM, Yin L, Ohashi-Doi K, Habgood M, Bron R, Brock JA, Gale JD, Furness JB (2010b) Evidence for functional ghrelin receptors on parasympathetic preganglionic neurons of micturition control pathways in the rat. Clin Exp Pharmacol Physiol 37:926–932.

Fick LJ, Fick GH, Belsham DD (2010) Rhythmic clock and neuropeptide gene expression in hypothalamic mHypoE-44 neurons. Mol Cell Endocrinol 323:298–306.

Fry M, Ferguson AV (2009) Ghrelin modulates electrical activity of area postrema neurons. Am J Physiol 296:R485–R492.

Furness JB, Costa M, Gibbins IL, Llewellyn-Smith IJ, Oliver JR (1985) Neurochemically similar myenteric and submucous neurons directly traced to the mucosa of the small intestine. Cell Tissue Res 241:155–163.

Gahete MD, Rubio A, Córdoba-Chacón J, Gracia-Navarro F, Kineman RD, Avila J, Luque RM, Castaño JP (2010) Expression of the ghrelin and neurotensin systems is altered in the temporal lobe of Alzheimer's disease patients. J Alzheimers Dis 22:819–828.

Grouselle D, Chaillou E, Caraty A, Bluet-Pajot MT, Zizzari P, Tillet Y, Epelbaum J (2008) Pulsatile cerebrospinal fluid and plasma ghrelin in relation to growth hormone secretion and food intake in the sheep. J Neuroendocrinol 20:1138–1146.

Guan XM, Yu H, Palyha OC, McKee KK, Feighner SD, Sirinathsinghji DJ, Smith RG, Van der Ploeg LH, Howard AD (1997) Distribution of mRNA encoding the growth hormone secretagogue receptor in brain and peripheral tissues. Brain Res Mol Brain Res 48:23–29.

Heimer GV, Taylor CE (1974) Improved mountant for immunofluorescence preparations. J Clin Pathol 27:254–256.

Hewson AK, Dickson SL (2000) Systemic administration of ghrelin induces Fos and Egr-1 proteins in the hypothalamic arcuate nucleus of fasted and fed rats. J Neuroendocrinol 12:1047–1049.

Hirayama H, Shiina T, Shima T, Kuramoto H, Takewaki T, Furness JB, Shimizu Y (2010) Contrasting effects of ghrelin and des-acyl ghrelin on the lumbo-sacral defecation center and regulation of colorectal motility in rats. Neurogastroenterol Motil 22:1124–1131.

Hökfelt T, Johansson O, Goldstein M (1984) Chemical anatomy of the brain. Science 225:1326–1334.

Holst B, Schwartz TW (2004) Constitutive ghrelin receptor activity as a signaling set-point in appetite regulation. Trends Pharmacol Sci 25:113–117.

Hosoda H, Kojima M, Matsuo H, Kangawa K (2000) Ghrelin and des-acyl ghrelin: two major forms of rat ghrelin peptide in gastrointestinal tissue. Biochem Biophys Res Commun 279:909–913.

Kageyama H, Kitamura Y, Hosono T, Kintaka Y, Seki M, Takenoya F, Hori Y, Nonaka N, Arata S, Shioda S (2008) Visualization of ghrelin-producing neurons in the hypothalamic arcuate nucleus using ghrelin-EGFP transgenic mice. Regul Pept 145:116–121.

Kineman RD, Gahete MD, Luque RM (2007) Identification of a mouse ghrelin gene transcript that contains intron 2 and is regulated in the pituitary and hypothalamus in response to metabolic stress. J Mol Endocrinol 38:511–521.

Kojima M, Hosoda H, Date Y, Nakazato M, Matsuo H, Kangawa K (1999) Ghrelin is a growth-hormone-releasing acylated peptide from stomach. Nature 402:656–660.

Lin Y, Matsumura K, Fukuhara M, Kagiyama S, Fujii K, Iida M (2004) Ghrelin acts at the nucleus of the solitary tract to decrease arterial pressure in rats. Hypertension 43:977–982.

Ljungdahl A, Hökfelt T, Nilsson G (1978) Distribution of substance P-like immunoreactivity in the central nervous system of the rat-I. Cell bodies and nerve terminals. Neuroscience 3:861–943.

Lu S, Guan JL, Wang QP, Uehara K, Yamada S, Goto N, Date Y, Nakazato M, Kojima M, Kangawa K, Shioda S (2002) Immunocytochemical observation of ghrelin-containing neurons in the rat arcuate nucleus. Neurosci Lett 321:157–160.

Lutter M, Sakata I, Osborne-Lawrence S, Rovinsky SA, Anderson JG, Jung S, Birnbaum S, Yanagisawa M, Elmquist JK, Nestler EJ, Zigman JM (2008) The orexigenic hormone ghrelin defends against depressive symptoms of chronic stress. Nat Neurosci 11: 752–753.

Menyhért J, Wittmann G, Hrabovszky E, Szlávik N, Keller E, Tschöp M, Liposits Z, Fekete C (2006) Distribution of ghrelin-immunoreactive neuronal networks in the human hypothalamus. Brain Res 1125:31–36.

Mitchell V, Bouret S, Beauvillain JC, Schilling A, Perret M, Kordon C, Epelbaum J (2001) Comparative distribution of mRNA encoding the growth hormone secretagogue-receptor (GHS-R) in Microcebus murinus (Primate, lemurian) and rat forebrain and pituitary. J Comp Neurol 429:469–489.

Mizutani M, Atsuchi K, Asakawa A, Matsuda N, Fujimura M, Inui A, Kato I, Fujimiya M (2009) Localization of acyl ghrelin- and des-acyl ghrelin-immunoreactive cells in the rat stomach and their responses to intragastric pH. Am J Physiol 297:G974–G980.

Mondal MS, Date Y, Yamaguchi H, Toshinai K, Tsuruta T, Kangawa K, Nakazato M (2005) Identification of ghrelin and its receptor in neurons of the rat arcuate nucleus. Regul Pept 126:55–59.

Nakazato M, Murakami N, Date Y, Kojima M, Matsuo H, Kangawa K, Matsukura S (2001) A role for ghrelin in the central regulation of feeding. Nature 409:194–198.

Patterson M, Murphy KG, le Roux CW, Ghatei MA, Bloom SR (2005) Characterization of ghrelin-like immunoreactivity in human plasma. J Clin Endocrinol Metab 90:2205–2211.

Perello M, Sakata I, Birnbaum S, Chuang JC, Osborne-Lawrence S, Rovinsky SA, Woloszyn J, Yanagisawa M, Lutter M, Zigman JM (2010) Ghrelin increases the rewarding value of high-fat diet in an orexin-dependent manner. Biol Psychiatry 67:880–886.

Sakata I, Nakano Y, Osborne-Lawrence S, Rovinsky SA, Lee CE, Perello M, Anderson JG, Coppari R, Xiao G, Lowell BB, Elmquist JK, Zigman JM (2009) Characterization of a novel ghrelin cell reporter mouse. Regul Pept 155:91–98.

Sasek CA, Seybold VS, Elde RP (1984) The immunohistochemical localization of nine peptides in the sacral parasympathetic nucleus and the dorsal gray commissure in rat spinal cord. Neuroscience 12:855–873.

Sato T, Fukue Y, Teranishi H, Yoshida Y, Kojima M (2005) Molecular forms of hypothalamic ghrelin and its regulation by fasting and 2-deoxy-D-glucose administration. Endocrinology 146:2510–2516.

Seim I, Josh P, Cunningham P, Herington A, Chopin L (2011) Ghrelin axis genes, peptides and receptors: recent findings and future challenges. Mol Cell Endocrinol 340:3–9.

Shimizu Y, Chang EC, Shafton AD, Ferens DM, Sanger GJ, Witherington J, Furness JB (2006) Evidence that stimulation of ghrelin receptors in the spinal cord initiates propulsive activity in the colon of the rat. J Physiol (Lond) 576:329–338.

Tsubota Y, Owada-Makabe K, Yukawa K, Maeda M (2005) Hypotensive effect of des-acyl ghrelin at nucleus tractus solitarii of rat. Neuroreport 16:163–166.

Turek FW, Joshu C, Kohsaka A, Lin E, Ivanova G, McDearmon E, Laposky A, Losee-Olson S, Easton A, Jensen DR, Eckel RH, Takahashi JS, Bass J (2005) Obesity and metabolic syndrome in circadian *Clock* mutant mice. Science 308:1043–1045.

Wortley KE, Anderson KD, Garcia K, Murray JD, Malinova L, Liu R, Moncrieffe M, Thabet K, Cox HJ, Yancopoulos GD, Wiegand SJ, Sleeman MW (2004) Genetic deletion of ghrelin does not decrease food intake but influences metabolic fuel preference. Proc Natl Acad Sci U S A 101:8227–8232.

Zhang J, Liu S, Tang M, Chen JD (2008) Optimal locations and parameters of gastric electrical stimulation in altering ghrelin and oxytocin in the hypothalamus of rats. Neurosci Res 62:262–269.

Zigman JM, Jones JE, Lee CE, Saper CB, Elmquist JK (2006) Expression of ghrelin receptor mRNA in the rat and the mouse brain. J Comp Neurol 494:528–548.

(Accepted 25 July 2011)
(Available online 31 July 2011)

Review

Digestion

Digestion 2012;85:90–94
DOI: 10.1159/000334654

Published online: January 19, 2012

Regulation of Gastroduodenal Motility: Acyl Ghrelin, Des-Acyl Ghrelin and Obestatin and Hypothalamic Peptides

Mineko Fujimiya[a] Koji Ataka[a] Akihiro Asakawa[b] Chih-Yen Chen[d] Ikuo Kato[c] Akio Inui[b]

[a]Department of Anatomy, Sapporo Medical University School of Medicine, Sapporo, [b]Department of Behavioral Medicine, Kagoshima University Graduate School of Medical and Dental Sciences, Kagoshima, and [c]Department of Bioorganic Chemistry, Faculty of Pharmaceutical Sciences, Hokuriku University, Kanazawa, Japan; [d]Faculty of Medicine, National Yang-Ming University School of Medicine, and Division of Gastroenterology, Department of Medicine, Taipei Veterans General Hospital, Taipei, Taiwan, ROC

Key Words
Gastroduodenal motility, regulation · Acyl ghrelin · Des-acyl ghrelin · Obestatin · Hypothalamic peptides

Abstract
Real-time measurements for gut motility in conscious rats or mice combined with intracerebroventricular or intravenous injection of peptide agonists or antagonists allow us to understand the regulatory mechanism of gastrointestinal motility. Neuropeptide Y (NPY) in the arcuate nucleus in the hypothalamus stimulates the fasted motility in the duodenum, while urocortin in the paraventricular nucleus inhibits fed and fasted motility in the antrum and duodenum. Acyl ghrelin exerts stimulatory effects on the motility of the antrum and duodenum in both the fed and fasted state of animals. NPY Y2 and Y4 receptors in the brain may mediate the action of acyl ghrelin, and vagal afferent pathways might be involved in this mechanism. Des-acyl ghrelin exerts inhibitory effects on the motility of the antrum but not on the motility of the duodenum in the fasted state of animals. CRF type 2 receptor in the brain may mediate the action of des-acyl ghrelin, and vagal afferent pathways might not be involved in this mechanism. Obestatin exerts inhibitory effects on the motility of the antrum and duodenum in the fed state but not in the fasted state of animals. CRF type 1 and type 2 receptors in the brain may mediate the action of obestatin, and vagal afferent pathways might be partially involved in this mechanism.

Experimental Design for Studying Gastrointestinal Motility and Brain-Gut Axis

Although the regulation of hypothalamic peptides on feeding behavior or energy expenditure has been well established, the regulation on the gastrointestinal (GI) motility has not been fully understood. The detailed studies on the brain-gut axis are somewhat hampered by the methodological difficulties in directly measuring the GI motility in conscious animals with intracerebroventricular (ICV) injection of peptide agonists or antagonists.

We developed a freely moving conscious animal model to measure the GI motility in rats [1] and mice [2], combined with intravenous (IV) or ICV injection. This model permits the real-time measurements of GI motility in

KARGER

Fax +41 61 306 12 34
E-Mail karger@karger.ch
www.karger.com

0012–2823/12/0852–0090$38.00/0

Accessible online at:
www.karger.com/dig

Mineko Fujimiya
Department of Anatomy
Sapporo Medical University School of Medicine
Sapporo 060-8556 (Japan)
Tel. +81 11 611 2111, E-Mail fujimiya@sapmed.ac.jp

animals in the physiological fed and fasted states under stimulation of the brain or peripheral administration of peptide agonists or antagonists. In the fasted state, the cyclic change of pressure waves were detected in both antrum and duodenum, including the quiescence period during which relatively low amplitude contractions occur (phase I-like contractions), followed by a grouping of strong contractions (phase III-like contractions). After food intake, such a fasted motor pattern was disrupted and replaced by a fed motor pattern, which consisted of irregular contractions of high frequency. By using this method the effects of brain-gut peptides on the GI motility can be examined.

Neuropeptide Y and Urocortin in the Hypothalamus Regulate the Gastroduodenal Motility

Neuropeptide Y (NPY) is a potent feeding-stimulatory peptide that expresses in the arcuate nucleus of the hypothalamus and projects predominantly to the paraventricular nucleus. Because few previous studies have examined the effects of centrally administered NPY-related peptide on GI motility, we investigated the role of NPY in the control of GI motility using a variety of NPY analogs [1]. ICV injection of Y2 and Y4 receptor agonists induced the phase III-like contractions in the duodenum when given in the fed state of rats; however, Y1 and Y5 receptor agonists had no effects on the motility despite their potent feeding-stimulatory effects [1]. More interestingly, immunoneutralization of NPY by ICV injection of NPY antibody completely blocked the phase III-like contractions in the duodenum [1]. This finding suggests that the fasted motor activity in the upper GI tracts is regulated by brain NPY neurons but not regulated by peripheral mechanism.

CRF and endogenous CRF receptor ligand urocortin are feeding-inhibitory peptides localized at the paraventricular nucleus in the hypothalamus. Urocortin binds both CRF type 1 and 2 receptors but shows a higher affinity for CRF type 2 receptor than type 1 receptor. CRF type 2 receptors are related to the stress-induced alterations of GI functions. ICV or IV injection of urocortin disrupted fasted motor activity in both antrum and duodenum, which were replaced by fed-like motor patterns [3]. When urocortin was given ICV in the fed state, the % motor index (%MI) was decreased in the antrum and increased in the duodenum [3]. Increase the %MI in the duodenum was non-propagated and therefore urocortin suppressed the transit of intestinal contents [3].

Colocalization of Acyl Ghrelin, Des-Acyl Ghrelin and Obestatin in Endocrine Cells in the Stomach

Acyl ghrelin was first isolated from rat and human stomach [4], and the localization of acyl ghrelin in the stomach was studied in various animals by using the specific antibody for acyl ghrelin [4, 5]; however, the localization of des-acyl ghrelin in the stomach has scarcely been examined. Our group developed antibodies specific for acyl ghrelin (anti-rat octanoyl ghrelin (1–15)-cys-KLH serum) and for des-acyl ghrelin (anti-rat des-octanoyl ghrelin (1–15)-cis-KLH serum) and successfully detected the different localization of acyl ghrelin and des-acyl ghrelin in the rat stomach [6].

Both acyl ghrelin- and des-acyl ghrelin-immunoreactive cells were distributed in the oxyntic and antral mucosa of the rat stomach, with higher density in the antral mucosa than oxyntic mucosa. Immunofluorescence double staining showed that acyl ghrelin- and des-acyl ghrelin-positive reactions overlapped in closed-type round cells, whereas des-acyl ghrelin-positive reaction was found in open-type cells in which acyl ghrelin was negative (fig. 1a). Acyl ghrelin/des-acyl ghrelin-positive closed-type cells contain obestatin (fig. 1b), on the other hand, des-acyl ghrelin-positive open-type cells contain somatostatin [6].

It is possible that open-type cells may react to luminal stimuli more than closed-type cells. Therefore, we investigated the effects of different intragastric pH levels on the release of acyl ghrelin and that of des-acyl ghrelin from the ex vivo perfused rat stomach [6]. The results showed that the release of acyl ghrelin was not affected by intragastric pH, whereas the release of des-acyl ghrelin was increased at intragastric pH 2 compared to that at intragastric pH 4 [6]. Therefore, the release of des-acyl ghrelin is stimulated after meals by lowering the intragastric pH. The release of acyl ghrelin, on the other hand, is stimulated before meals and the release is regulated by plasma levels of glucose and insulin [7].

Regulation of Acyl Ghrelin on the Gastroduodenal Motility

We examined the effects of acyl ghrelin on the gastroduodenal motility and involvement of hypothalamic peptides mediating this action. Acyl ghrelin stimulated the %MI in the antrum and induced the fasted motor activity in the duodenum when given in the fed state of animals [8]. Acyl ghrelin increased the frequency of phase

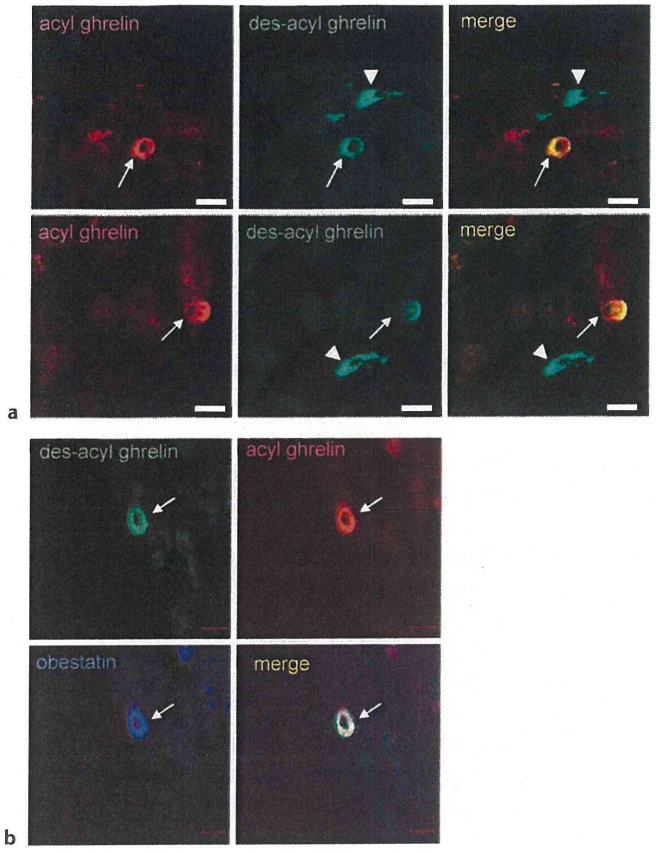

Fig. 1. Localization of acyl ghrelin, des-acyl ghrelin and obestatin in the rat stomach. **a** Immunofluorescence double staining for acyl ghrelin- (red) and des-acyl ghrelin-positive (green) reaction in the antral mucosa of rat stomach. Acyl ghrelin-positive reaction and des-acyl ghrelin-positive reaction are colocalized in closed-type cells (arrows), whereas des-acyl ghrelin-positive reaction is localized in open-type cells (arrowheads). **b** Immunofluorescence triple staining for des-acyl ghrelin (green), acyl ghrelin (red) and obestatin (blue) in the antral mucosa of rat stomach. Three peptides are colocalized in the closed-type cells (arrows). Bars = 10 μm [from 6].

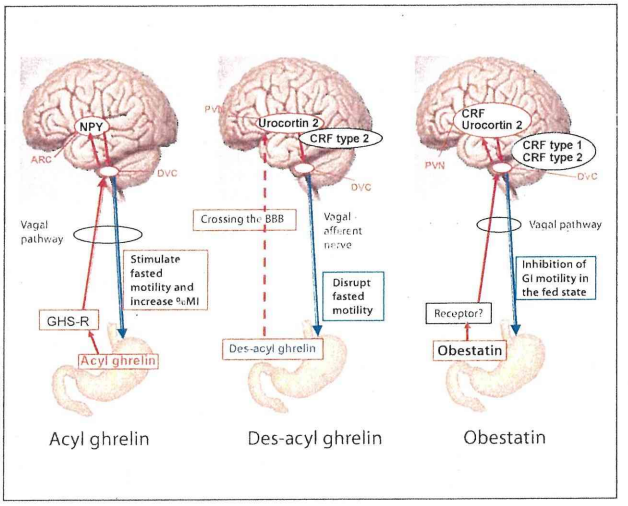

Fig. 2. Different pathways of acyl ghrelin, des-acyl ghrelin and obestatin. Acyl ghrelin released from the endocrine cells in the stomach may act on the ghrelin receptor on vagal afferent nerve terminals, and NPY neurons in the arcuate nucleus may mediate the action of acyl ghrelin to stimulate gastroduodenal motility. Des-acyl ghrelin released from endocrine cells in the stomach may activate urocortin-2 neurons in the paraventricular nucleus by crossing the BBB, and exert inhibitory effects on the antral motility via CRF type 2 receptor in the brain. Obestatin may act on the obestatin receptor on vagal afferent nerve terminals, and CRF and urocortin-2 neurons in the paraventricular nucleus may mediate the action of obestatin to inhibit the gastroduodenal motility via CRF type 1 and type 2 receptors in the brain.

III-like contractions in both antrum and duodenum when given in the fasted state of animals [8]. The effects of IV injection of acyl ghrelin on gastroduodenal motility were blocked by IV injection of GHS-R antagonist [8]. Immunoneutralization of NPY in the brain blocked the stimulatory effects of acyl ghrelin on the gastroduodenal motility [8]. These results indicate that acyl ghrelin released from the stomach may act on the ghrelin receptor on vagal afferent nerve terminals and NPY neurons in the brain may mediate the action of acyl ghrelin on the gastroduodenal motility. Taken together, in normal animals, acyl ghrelin may stimulate gastroduodenal motility by activating the GHS-R on vagal afferent nerve terminals and affect NPY neurons in the hypothalamus, Y2 and/or Y4 receptors in the brain may mediate the action of acyl ghrelin (fig. 2; table 1).

Regulation of Des-Acyl Ghrelin on the Gastroduodenal Motility

Des-acyl ghrelin disrupted fasted motility in the antrum but not in the duodenum; however, des-acyl ghrelin did not alter fed motor activity in both the antrum and duodenum [9]. Capsaicin treatment did not alter the disruptive effect of IV injection of des-acyl ghrelin on fasted motility in the antrum [9]. These results suggest that peripherally administered des-acyl ghrelin may cross the blood-brain barrier (BBB) and act directly on

Table 1. Comparison of the effects of acyl ghrelin, des-acyl ghrelin and obestatin on the gastroduodenal motility

	Acyl ghrelin		Des-acyl ghrelin		Obestatin	
	fasted motility	fed motility	fasted motility	fed motility	fasted motility	fed motility
Stomach	↑	↑	↓	–	–	↓
Duodenum	↑	↑	–	–	–	↓
Hypothalamic neuron	NPY		Urocortin-2		CRF, urocortin-2	
Brain receptor	Y2, Y4		CRF type 2		CRF type 1, type 2	
Vagal afferent pathway	+		–		+	

the brain receptor and disrupt the fasted motility in the antrum.

The centrally administered CRF type 2 receptor antagonist, but not the CRF type 1 receptor antagonist, blocked the effects of centrally and peripherally administered des-acyl ghrelin on gastric motility [9]. The density of c-*Fos*-positive cells in the PVN was significantly increased by intraperitoneal injection of des-acyl ghrelin compared to vehicle-injected controls [9]. These data suggest that peripherally administered des-acyl ghrelin may activate neurons in the PVN by crossing the BBB, and exert inhibitory effects on the antral motility via CRF type 2 receptor in the brain (fig. 2; table 1).

Regulation of Obestatin on the Gastroduodenal Motility

Most of the previous studies have shown the negative effects of obestatin on the GI motility; in those studies, however, only the gastric emptying or MMC cycle time has been used as indices for motor activity. We obtained the positive effects of obestatin on the gastroduodenal motility by analyzing the motor activity in fed and fasted states, and measuring the time taken to the initiation of phase III-like contractions in the antrum and duodenum of conscious rats [10].

Obestatin decreased the %MI of fed motility in the antrum and prolonged the time before the return of fasted motility in the duodenum [10]. IV injection of obestatin induced a significant increase in the number of c-*Fos*-positive cells in the PVN compared to saline-injected controls [10]. Immunofluorescence overlap staining showed that the PVN neurons activated by IV injection of obestatin contain CRF or urocortin-2 [10]. The inhibitory action of IV injection of obestatin on the motor activities in the antrum and duodenum were blocked by ICV injection of CRF type 1 and type 2 receptor antagonists, suggesting that both types of CRF receptors in the brain may mediate the action of peripherally injected obestatin on gastroduodenal motility [10]. Combined together, obestatin inhibits gastroduodenal motility in the fed state but not in the fasted state of conscious rats. In the brain, CRF- and urocortin-2-containing neurons might be activated by IV injection of obestatin, and at the level, CRF type 1 and type 2 receptors might be involved in the inhibitory action of obestatin on antral and duodenal motility. Vagal afferent pathways might be involved partially, but not entirely, in these actions of obestatin (fig. 2; table 1).

Conclusions

Acyl ghrelin, des-acyl ghrelin and obestatin are included in the endocrine cells in the stomach and regulate the upper GI motility by activating hypothalamic peptides [11, 12]. Since hypothalamic peptides are strongly affected by stress or anxiety, such brain-gut interaction seems to be important to understand the pathogenesis of functional disorder in the GI tracts.

Disclosure Statement

The authors declare that no financial or other conflict of interest exists in relation to the content of the article.

References

1 Fujimiya M, Itoh E, Kihara N, Yamamoto I, Fujimura M, Inui A: Neuropeptide Y induces fasted pattern of duodenal motility via Y2 receptors in conscious fed rats. Am J Physiol Gastrointest Liver Physiol 2000;278:G32–G38.

2 Tanaka R, Inui A, Asakawa A, Atsuchi K, Ataka K, Fujimiya M: New method of manometric measurement of gastroduodenal motility in conscious mice: effects of ghrelin and Y2 depletion. Am J Physiol Gastrointest Liver Physiol 2009;297:G1028–G1034.

3 Kihara N, Fujimura M, Yamamoto I, Itoh E, Inui A, Fujimiya M: Effect of central and peripheral urocortin on fed and fasted gastroduodenal motor activity in conscious rats. Am J Physiol Gastrointest Liver Physiol 2001; 280:G406–G419.

4 Kojima M, Hosoda H, Date Y, Nakazato M, Matsuo H, Kangawa K: Ghrelin is a growth-hormone-releasing acylated peptide from stomach. Nature 1999;402:656–660.

5 Sakata I, Mori T, Kaiya H, Yamazaki M, Kangawa K, Inoue K, Sakai T: Localization of ghrelin-producing cells in the stomach of the rainbow trout *(Oncorhynchus mykiss).* Zoolog Sci 2004;21:757–762.

6 Mizutani M, Atsuchi K, Asakawa A, Matsuda N, Fujimura M, Inui A, Kato I, Fujimiya M: Localization of acyl ghrelin- and des-acyl ghrelin-immunoreactive cells in the rat stomach and their responses to intragastric pH. Am J Physiol Gastrointest Liver Physiol 2009;297:G974–G980.

7 Chen CY, Asakawa A, Fujimiya M, Lee SD, Inui A: Ghrelin gene products and the regulation of food intake and gut motility. Phamacol Rev 2009;61:430–481.

8 Fujino K, Inui A, Asakawa A, Kihara N, Fujimura M, Fujimiya M: Ghrelin-induced fasted motor activity of the gastrointestinal tract in conscious fed rats. J Physiol 2003; 550:227–240.

9 Chen CY, Inui A, Asakawa A, Fujino K, Kato K, Chen CC, Ueno N, Fujimiya M: Des-acyl ghrelin acts by CRF type 2 receptors to disrupt fasted stomach motility in conscious rats. Gastroenterology 2005;129:8–25.

10 Ataka K, Inui A, Asakawa A, Kato I, Fujimiya M: Obestatin inhibits motor activity in the antrum and duodenum in the fed state of conscious rats. Am J Physiol Gastrointest Liver Physiol 2008;294:G1210–G1218.

11 Fujimiya M, Asakawa A, Ataka A, Kato I, Inui A: Different effects of ghrelin, des-acyl ghrelin and obestatin on gastroduodenal motility in conscious rats. World J Gastroenterol 2008;14:6318–6326.

12 Fujimiya M, Asakawa A, Ataka K, Chen CY, Kato I, Inui A: Ghrelin, des-acyl ghrelin, and obestatin: regulatory roles on the gastrointestinal motility. Int J Pept 2010;2010. pii: 305192.

Biochemical and Biophysical Research Communications 407 (2011) 557–561

Contents lists available at ScienceDirect

Biochemical and Biophysical Research Communications

journal homepage: www.elsevier.com/locate/ybbrc

An Mdm2 antagonist, Nutlin-3a, induces p53-dependent and proteasome-mediated poly(ADP-ribose) polymerase1 degradation in mouse fibroblasts

Shingo Matsushima [1], Naoyuki Okita [*,1], Misako Oku, Wataru Nagai, Masaki Kobayashi, Yoshikazu Higami [*]

Department of Molecular Pathology and Metabolic Disease, Faculty of Pharmaceutical Sciences, Tokyo University of Science, Yamazaki 2641, Noda, Chiba 278-0022, Japan

ARTICLE INFO

Article history:
Received 10 March 2011
Available online 16 March 2011

Keywords:
Nutlin-3a
Poly(ADP-ribose) polymerase1
p53
Mdm2
Proteasome

ABSTRACT

Nutlin-3a (Nutlin) is an Mdm2 inhibitor and is potent to stabilize p53, which is a tumor-suppressor involved in various biological processes such as cell cycle regulation, DNA repair, and apoptosis. Here we demonstrate that Nutlin treatment in mouse fibroblast cell lines reduces the protein levels of poly(ADP-ribose) polymerase1 (Parp1). Parp1 functions in DNA repair, replication, and transcription and has been regarded as a target molecule for anti-cancer therapy and protection from ischemia/reperfusion injury. In this study, first we found that Nutlin, but not DNA damaging agents such as camptothecin (Cpt), induced a decrease in the Parp1 protein levels. This reduction was not associated with cell death and not observed in p53 deficient cells. Next, because Nutlin treatment did not alter Parp1 mRNA levels, we expected that a protein degradation pathway might contribute to this phenomenon. Predictably, a proteasome inhibitor, MG132, inhibited the Nutlin-induced decrease in the levels of Parp1 protein. These results show that Nutlin induces the proteasomal degradation of Parp1 in a p53-dependent manner. Thus, this study demonstrates characterization of a novel regulatory mechanism of Parp1 protein. This novel regulatory mechanism of Parp1 protein level could contribute to development of inhibitors of the Parp1 signaling pathway.

1. Introduction

p53 is a tumor-suppressor that is mutated or deleted in more than half of all human tumors. The physiological roles of p53 are versatile, forming a cell cycle checkpoint and functioning in DNA repair, apoptosis, and energy metabolism [1]. It has been shown that phosphorylations at multiple sites and subsequent proteasomal degradation are important in the regulation of p53 protein levels [2]. p53 ubiquitination required in its degradation is catalyzed by several ubiquitin ligases such as Mdm2, Pirh2, and Cop1 [3]. In particular, the regulatory mechanism of p53 by Mdm2 has been well-analyzed. Because the massive stabilization of p53 was able to induce apoptosis in p53 proficient tumor cells [4], stabilization of p53 via an inhibition of Mdm2 is one of the attractive strategies for cancer therapy. Recently, it has been reported that small molecular compounds such as Nutlin and MI-219 act as cell-permeable Mdm2 antagonists [5,6], and their analogs have progressed to preclinical development or early phase clinical trials for anti-cancer therapy [7].

Parp1 is a major enzyme catalyzing poly(ADP-ribosyl)ation, which is a post-translational protein modification. It is involved in replication, DNA repair, and cell death [8,9]. Parp1 is dramatically activated by DNA breaks and then catalyzes poly(ADP-ribosyl)ation on substrate proteins in DNA damage regions, which is required for efficient recruitment of DNA repair factors to the loci [10,11]. On the other hand, over-activation of Parp1 decreases cellular NAD^+ and ATP levels, resulting in necrotic cell death caused by breakdown of energy metabolism [12,13]. The involvement of Parp1 in inflammatory responses has also been reported. Ischemia/reperfusion-induced Parp1 over-activation is mediated by production of reactive oxygen species and is involved in NF-κB transactivation [14]. Furthermore, Parp1 has been also characterized as a useful hallmark of apoptosis because full length Parp-1 is cleaved by the apoptotic proteases, caspase-3 and -7, into p85 and p25 fragments during apoptosis [15,16]. Therefore, Parp1 is an attractive target of cancer chemotherapy and protection from ischemia/reperfusion injury, and several Parp1 inhibitors are being evaluated in clinical trials [17].

Recently, using Nutlin, we have analyzed p53 functions that are independent of DNA damage response and incidentally found that Parp1 proteins disappear in Nutlin-treated cells. In this study, we show the basic characterization of Nutlin-mediated Parp1 protein degradation and discuss the use of Nutlin as a Parp1 inhibitor for protection against ischemia/reperfusion injury and anti-cancer therapy.

* Corresponding authors. Fax: +81 4 7121 3676..
E-mail addresses: nokita7@rs.noda.tus.ac.jp (N. Okita), higami@rs.noda.tus.ac.jp (Y. Higami).
[1] These authors equally contributed to this work.

0006-291X/$ - see front matter © 2011 Elsevier Inc. All rights reserved.
doi:10.1016/j.bbrc.2011.03.061

2. Materials and methods

2.1. Cell culture and drugs

Mouse fibroblast cell line 3T3-L1 and 3T3-F442A were purchased from the RIKEN Bioresource Center (Japan) and the European Collection of Animal Cell Cultures (UK), respectively. p53 deficient mouse-derived fibroblast cell line HW [18] was kindly provided by Dr. Masayuki Saito (Tenshi University, Japan). The cells were maintained in Dulbecco's modified Eagle's medium (low glucose) (WAKO, Japan) with 10% fetal calf serum and 1% penicillin/streptomycin (SIGMA). Cpt and MG132 were purchased from WAKO (Japan). Nutlin was supplied by Cayman (USA).

2.2. p53 overexpression and knockdown

p53 cDNA was amplified from mouse liver cDNA by PCR using KOD plus (TOYOBO, Japan) and subcloned into EcoRV-digested pBluescript II SK(+). And then p53 cDNA fragment obtained by BamHI and DraI digestion of the subcloned vector were cloned into EcoRV and BamH1-digested pIRES-Neo3 (Clontech, USA). The produced vector, p53-IRES-Neo3, was transfected with Lipofectamine LTX (Invitrogen, USA) into 3T3-L1 cells, according to the manufacturer's protocol.

We designed a mouse p53 shRNA expression vector based on target sequences for effective p53 knockdown, as previously reported [19]. Two oligonucleotides, 5′-gatccccGTACGTGTGTAGTA GCTTCttcaagagaGGAGCTATTACACATGTACtttttggaaa-3′ and 5′-agc ttttccaaaaaGTACATGTGTAATAGCTCCtctcttgaaGAAGCTACTACACAC GTACggg -3′ (upper case letters, target sequences against p53; lower case letters, BglII, HindIII or loop structure sequences) were chemically synthesized (Operon Biotechnology, USA). The annealed oligos were directly ligated into a BglII and HindIII-digested pSUPER-puro shRNA expression vector gifted from Dr. Shigeo Ohno (Yokohama City University, Japan) [20]. The produced vector, termed pSUPER-puro-shmp53, was transfected with Lipofectamine LTX (Invitrogen, USA) into 3T3-L1 cells, according to the manufacturer's protocol. For stable p53 knockdown cell lines, the transfected cells were selected with puromycin and resistant clones were isolated by trypsinization using cloning cylinders.

2.3. Preparation of primary mouse embryonic fibroblasts (MEFs)

p53 heterozygous mice (Accession No. CDB 0001K) [21] were purchased from RIKEN BRC (Japan). p53 heterozygous males and females were crossed, and MEFs were prepared from the pregnant females. Each 13- to 15-day-old embryo was dissected from the uterus and washed with PBS. After removal of the head, tail, limbs, and blood-enriched organs, the trimmed embryo was washed with PBS and minced. After trypsinization at 37 °C for 10 min followed by inactivation of trypsin by addition of FCS, MEFs were separated by filtration through a cell-strainer. p53 status was confirmed by PCR using previously described primers (forward primer for p53 genomic sequence, 5′-AATTGACAAGTTATGCATCCAACAGTACA-3′; reverse primer for p53 genomic sequence, 5′-ACTCCTCAACATC CTGGGGCAGCAACAGAT-3′, forward primer for neo sequence, 5′-GAACCTGCGTGCAATCCATCTTGTTCAATG-3′) [21] and the established MEFs were maintained in DMEM high glucose with 10% FCS, 2-mercaptoethanol (2-ME), and antibiotics.

2.4. Western blotting

Cells were lyzed by the addition of lysis buffer (50 mM Tris–HCl pH6.8, 2% SDS, 5% glycerol), boiled for 5 min, and sonicated. Protein concentrations of the soluble fraction were determined by BCA protein assay (PIERCE, USA) according to the manufacturer's protocol, and standardized by the addition of lysis buffer. Following this, the proteins were added to 2-ME and bromophenol blue so as to obtain final concentrations of 5% and 0.025%, respectively, and boiled for 5 min. Equal amounts of proteins (5–20 μg) were subjected to SDS–PAGE and transferred to nitrocellulose membranes. The membranes were blocked with 2.5% skim milk and 0.25% BSA in TBS (50 mM Tris, pH 7.4, 150 mM NaCl) containing 0.1% Tween 20 (TTBS) for 1 h at room temperature, and then probed with appropriate primary antibodies overnight at 4 °C or for 2 h at room temperature. As primary antibodies, anti-Parp1 (clone C-2-10, WAKO, Japan), anti-p53 (clone Ab-1, Calbiochem, USA), anti-b actin (clone AC-15, SIGMA, USA), or anti-caspase-3 (clone 1F3, MBL, Japan) antibodies were used. After washes with TTBS, the membranes were incubated with the appropriate secondary antibody, horseradish peroxidase-conjugated $F(ab')_2$ fragment of goat anti-mouse IgG or anti-rabbit IgG (Jackson Immunoresearch, USA), for 1 h at room temperature. After washing the membrane with TTBS, the membranes were incubated with ImmunoStar LD reagent (WAKO, Japan). The specific proteins were visualized with LAS3000 (FUJI FILM, Japan), and the data were analyzed using MultiGauge software (FUJI FILM, Japan).

2.5. RNA purification and RT-PCR

Cells were lyzed by RNAiso PLUS (TaKaRa, Japan), and then total RNA was purified using a FastPure RNA kit (TaKaRa, Japan) according to manufacturer's protocol. Purified RNA (1 μg) was subjected to reverse transcription with PrimeScript Reverse Transcriptase (TaKaRa, Japan) and random hexamer (TaKaRa, Japan). The PCR reaction was performed using Platinum Taq DNA Polymerase High Fidelity (Invitrogen, USA) and *Parp1* (forward, 5′-TGCTCATCTT CAACCAGCAG-3′; reverse, 5′-TCCTTTGGAGTTACCCATTCC-3′) or β-*actin* primers (forward, 5′-TCTTTGCAGCTCCTTCGTTG-3′; reverse, 5′-GGCCTCGTCACCCACATAG-3′) as follows: initiation step, at 94 °C for 1 min; amplification step, 30 (*Parp-1*) or 25 (*b-actin*) cycles of at 94 °C for 1 min, at 52 °C (*Parp-1*) or 61 °C (β-*actin*) for 15 s, at 68 °C for 15 s; termination step, 68 °C 15 s. PCR products were subjected to 1.8% agarose gel electrophoresis, stained with ethidium bromide, and visualized with LAS3000. The data was analyzed using MultiGauge software (FUJI FILM, Japan).

3. Results

3.1. Nutlin induces a decrease in parp1 protein levels in mouse fibroblast cell lines

When analyzing proteins of the Nutlin-treated mouse embryonic fibroblasts (MEFs), we observed a significant reduction in the levels of full length of Parp1 protein without cleavage into p85 and p25 apoptotic fragments (data not shown). Interestingly, under this condition, a trypan blue exclusion assay and images of phase-contrast microscope showed that the cells were viable, suggesting that the reduction of Parp1 protein was independent of cell death. Furthermore, because MEFs were induced apoptosis by staurosporine treatment, MEFs were responsive to apoptotic stimuli (data not shown). To examine whether p53 stabilization induces the decrease in Parp1 protein, 3T3-L1 and 3T3-F442A mouse fibroblast cells were treated with a DNA damaging agent, Cpt, or Nutlin. As shown in Fig. 1A and B, in both cell lines, Cpt treatment did not alter the Parp-1 protein levels, and Nutlin markedly decreased it, although both drugs induced p53 stabilization. Furthermore, overexpression of p53 protein did not markedly affect Parp1 protein levels (Fig. 1C). Consistent with our previous observations, no caspase-3 activation, which is a hallmark of apop-

tosis, was detected in these conditions. Furthermore, trypan blue staining showed that the Nutlin treatment did not induced cell death (Supplementary data Fig. 1). The time course analysis showed that Parp1 protein diminished by a treatment with 25 μM Nutlin for 8 h (Fig. 1D). These results suggest that in mouse fibroblasts Nutlin induces the reduction of Parp1 protein in a cell death-independent manner.

3.2. p53 Mediates Nutlin-induced decrease in parp1 protein

Since Nutlin stabilizes p53 *via* inhibition of Mdm2, we examined whether p53 contributes to the Nutlin-induced Parp-1 reduction. shRNA-mediated transient knockdown of p53 in 3T3-L1 cells attenuated the decrease in Parp1 by Nutlin treatment (Fig. 2A). Since p53 knockdown efficiency is not sufficient, we next analyzed this using two p53 deficient cell lines. 3T3-L1/shp53 cells were established by stable transfection with the pSUPER-puro-shmp53 plasmid vector followed by clone isolation, and its p53 protein expression levels were very much lower than in the transient knockdown. HW cells are a fibroblast cell line derived from p53 deficient mice. In these cell lines, the Nutlin-induced decrease in Parp1 was diminished significantly (Fig. 2B). Furthermore, we confirmed p53 dependency in the Nutlin-induced Parp1 reduction by using MEFs derived from p53+/+ or −/− mice, and obtained similar results (Fig. 2C). These results show that Nutlin reduces the Parp1 protein levels in a p53-dependent manner.

3.3. Nutlin-3 down-regulates parp-1 protein via proteasome

To examine whether the decrease in Parp1 protein by Nutlin treatment is caused by down-regulation of its mRNA, p53 proficient (3T3-L1 and 3T3-F442A) and deficient (3T3-L1/shp53 and HW) cell lines were treated with Nutlin, and then the Parp1 mRNA of each was analyzed by RT-PCR. Parp1 mRNA did not markedly change in either p53 proficient or deficient cell lines, even at doses of Nutlin where levels of Parp1 protein were completely dimin-

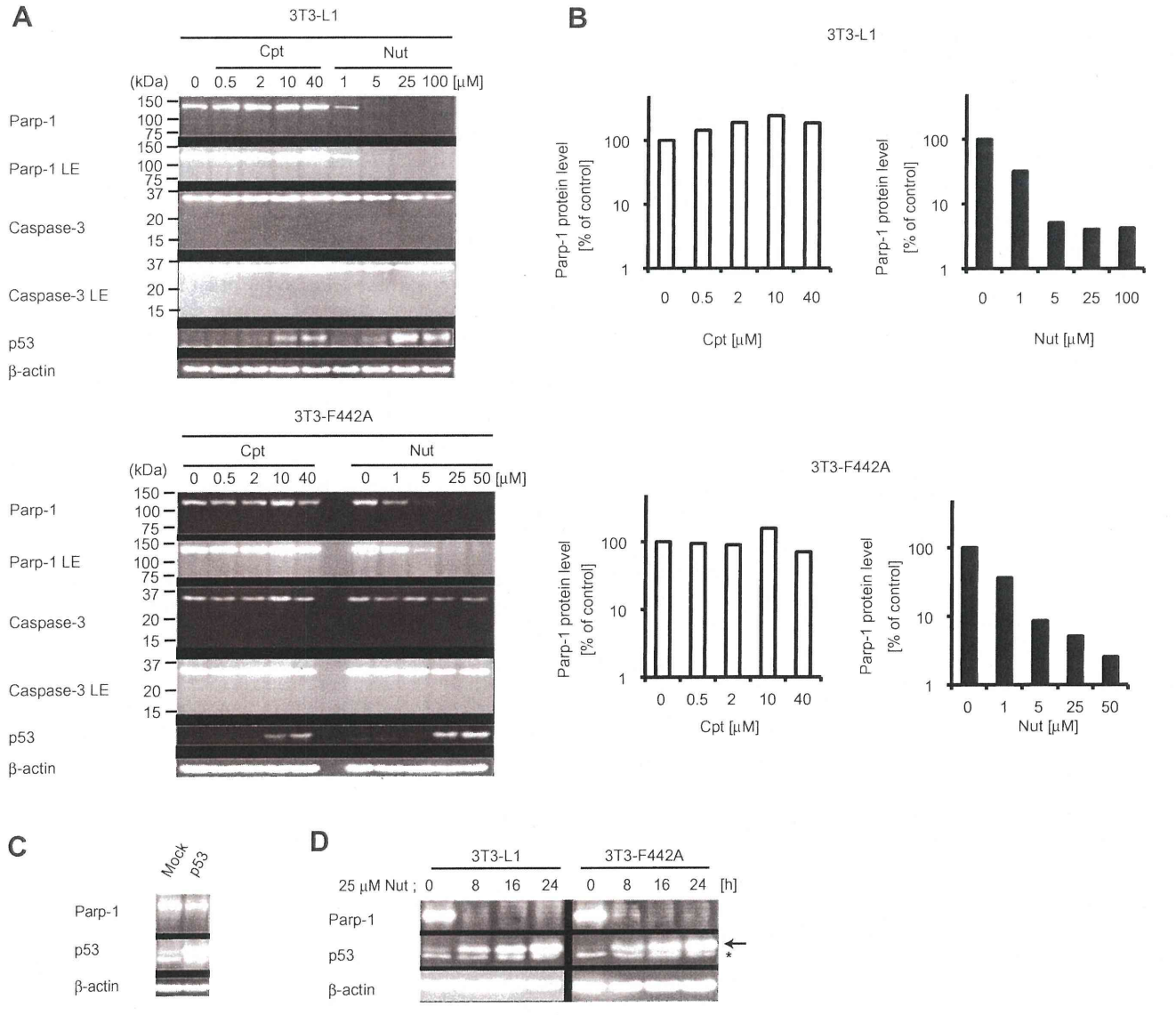

Fig. 1. Nutlin but not Cpt induces decrease in Parp1 protein levels in mammalian cell lines. A and B, mouse fibroblast 3T3-L1 (upper panel) or 3T3-F442A (lower panel) cells were treated with indicated concentrations of Cpt or Nutlin for 24 h. The cell lysates were analyzed by Western blotting using indicated antibodies (A). LE means long exposure. Quantitative data from (A) are shown (B). C, 3T3-L1 cells were transfected with mock or p53 expression vector. After transfection for 36 h, the cells were harvested and were analyzed by western blotting using indicated antibodies. D, 3T3-L1 or 3T3-F442A cells were treated with 25 μM Nutlin for the indicated times. Proteins were subjected to Western blotting. In the p53 panel, the arrow and asterisk show the p53 and nonspecific bands, respectively. All experiments were performed at least three times, and representative data are shown.

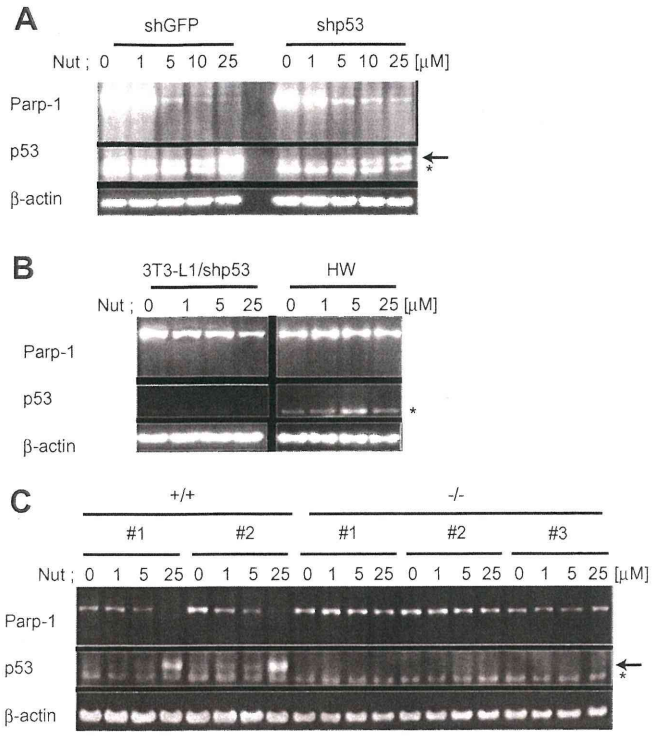

Fig. 2. Decrease in Parp1 protein levels induced by Nutlin is p53 status dependent. shGFP- and shp53- transiently transfected 3T3-L1 (A), HW, a mouse fibroblast cell line from p53 knockout mice, and 3T3-L1/shp53, a p53 stable knockdown cell line (B), and p53+/+ ($n = 2$) and p53−/− ($n = 3$) MEFs (C) were treated with indicated concentrations of Nutlin for 24 h. The cell lysates were analyzed by Western blotting using indicated antibodies. In the p53 panel, the arrow and asterisk show the p53 and nonspecific bands, respectively. All experiments were performed at least two times, and representative data are shown.

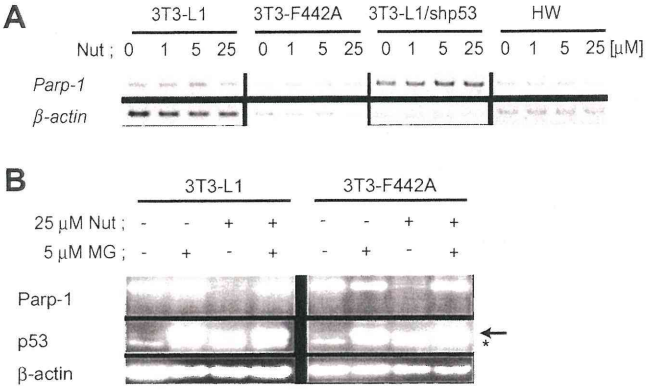

Fig. 3. Nutlin downregulates Parp-1 protein levels by proteasomal degradation. A, 3T3-L1, 3T3-F442A, 3T3-L1/shp53, and HW cells were treated with the indicated concentrations of Nutlin for 24 h. Parp1 mRNA was detected by RT-PCR. β-actin was used as a loading control. B, 3T3-L1 and 3T3-F442A cells were treated with 25 mM Nutlin in the presence or absence of 5 μM proteasome inhibitor MG132 (MG) for 8 h, and then the cell lysates were subjected to Western blotting using indicated antibodies. All experiments were performed at least three times, and representative data are shown.

ished (Fig. 3A). This result indicates that a decrease in Parp1 mRNA levels is not a main factor of Nutlin-induced Parp1 reduction. Therefore, we speculated that Nutlin-induced Parp1 reduction might involve proteasomal degradation. Thus, the effects of proteasome inhibition on Nutlin-induced Parp1 reduction were examined. Treatment with the proteasome inhibitor MG132 alone did not affect basal Parp1 protein levels, but it clearly inhibited the Nutlin-induced reduction in Parp1 (Fig. 3B). Taken together, these results indicate that the Nutlin treatment induced proteasome-mediated degradation of Parp-1 protein.

4. Discussion

In this study, we demonstrated that the Mdm2 inhibitor, Nutlin, induces the reduction of Parp1 protein by a p53-dependent mechanism. Interestingly, overexpression of p53 protein did not evoke a significant reduction in Parp1 protein, although that induced p53 accumulation similar to Nutlin. These results suggest that in the process of Nutlin-induced Parp1 reduction, p53 expression is required but is insufficient.

We examined whether the other commercially available Mdm2 inhibitors (NSC66811 [22] and trans-4-Iodo, 4′-boranyl-chalcone [23,24]) induced a reduction in Parp1 protein in 3T3-L1 cells. However, these Mdm2 inhibitors not only did not induce a reduction in Parp1 protein but also did not induce even p53 accumulation (data not shown). To conclude this issue, additional experiments would be required. We also showed that MG132 blocks the decrease in Parp1 protein. It was reported that Parp1 can be ubiquitinated *in vivo*, although it is unclear whether the ubiquitination is involved in proteasomal degradation of Parp1 [25]. Taken together with our findings, it is likely that the ubiquitin–proteasome pathway directly regulates the degradation of Parp1 protein.

In comparison to the many Parp1 inhibitors evaluated in ongoing clinical trials [17], the regulatory mechanism of Parp1 protein that we discovered provides some advantages. The first advantage is the novel mechanism of action as an inhibitor of the Parp1 signaling pathway. Because most of the Parp1-inhibiting compounds previously identified block the catalyzing activity of the protein, the specificity of these drugs in the other Parp family proteins that possess the highly conserved catalytic domain is a big issue [17]. On the other hand, Nutlin inhibits Parp1 signaling *via* induction of Parp1 protein degradation. Therefore, we expect that the inhibition specificity for Parp1 protein in the Parp family could be high. In any case, it is important to analyze the effects of Nutlin treatment on the protein levels of the other Parp family proteins. The second advantage is its cell type selectivity. In this paper, we demonstrated that in mouse fibroblasts Nutlin induces the decrease in Parp1 protein. On the other hand, it has been reported that Nutlin induces cleavage of Parp1 into two apoptotic fragments in the human colon cancer cell line, HCT116, and the human myeloid leukemia cell line, ML-1 [26,27]. In fact, we confirmed that there was no significant reduction in Parp1 protein other than apoptotic cleavage in HCT116 cells treated with various doses of Nutlin (data not shown). Furthermore, we have already examined responsiveness to Nutlin-induced Parp1 decrease in several human cell lines and have confirmed that human lung cancer cell line A549 were also responsive to Nutlin (data not shown). Taken together, we believe that Nutlin-induced Parp1 degradation has cell type selectivity. Moreover, considering co-treatment with DNA damaging agents for cancer therapy, Nutlin may reduce side effects caused by DNA damaging agents. It is well known that alkylating agents cause Parp1 over-activation, resulting in massive inflammation due to undesirable necrotic cell death caused by NAD^+ and ATP depletion [12,13], and that Parp1 is required for NF-κB transactivation, which is involved in inflammatory responses [14]. Therefore, co-treatment with Nutlin may also attenuate necrotic cell death and inflammation induced by Parp1 over-activation.

Thus, this study demonstrates characterization of a novel regulatory mechanism of Parp1 protein. The elucidation of the regulatory mechanism of Nutlin-induced elimination of Parp1 protein is important for the optimization of compounds inducing this phenomenon, resulting in establishment of selective chemotherapeutic strategies against ischemia/reperfusion injury and cancer.

Acknowledgments

The authors thank Dr. Masayuki Saito (Tenshi University, Japan) and Dr. Shigeo Ohno (Yokohama City University) for the provision of materials, and Natsumi Ishikawa for technical assistance. This project is partially supported by a research grant from Maekawa Houonkai (N.O.).

Appendix A. Supplementary data

Supplementary data associated with this article can be found, in the online version, at doi:10.1016/j.bbrc.2011.03.061.

References

[1] D.R. Green, G. Kroemer, Cytoplasmic functions of the tumor suppressor p53, Nature 458 (2009) 1127–1130.
[2] J.P. Kruse, W. Gu, Modes of p53 regulation, Cell 137 (2009) 609–622.
[3] T. Lee, W. Gu, The multiple levels of regulation by p53 ubiquitination, Cell Death Differ. 17 (2010) 86–92.
[4] E. Yonish-Rouach, D. Resnitzky, J. Lotem, L. Sachs, A. Kimchi, M. Oren, Wild-type p53 induces apoptosis of myeloid leukaemic cells that is inhibited by interleukin-6, Nature 352 (1991) 345–347.
[5] L.T. Vassilev, B.T. Vu, B. Graves, D. Carvajal, F. Podlaski, Z. Filipovic, N. Kong, U. Kammlott, C. Lukacs, C. Klein, N. Fotouhi, E.A. Liu, In vivo activation of the p53 pathway by small-molecule antagonists of MDM2, Science 303 (2004) 844–848.
[6] S. Shangary, D. Qin, D. McEachern, M. Liu, R.S. Miller, S. Qiu, Z. Nikolovska-Coleska, K. Ding, G. Wang, J. Chen, D. Bernard, J. Zhang, Y. Lu, Q. Gu, R.B. Shah, K.J. Pienta, X. Ling, S. Kang, M. Guo, Y. Sun, D. Yan, S. Wang, Temporal activation of p53 by a specific MDM2 inhibitor is selectively toxic to tumors and leads to complete tumor growth inhibition, Proc. Natl. Acad. Sci. USA 105 (2008) 3933–3938.
[7] S. Shangary, S. Wang, Small-molecule inhibitors of the MDM2–p53 protein-protein interaction to reactivate p53 function: a novel approach for cancer therapy, Annu. Rev. Pharmacol. Toxicol. 49 (2009) 223–241.
[8] M. Masutani, H. Nakagama, T. Sugimura, Poly(ADP-ribosyl)ation in relation to cancer and autoimmune disease, Cell. Mol. Life Sci. 62 (2005) 769–783.
[9] M. Miwa, M. Masutani, PolyADP-ribosylation and cancer, Cancer Sci. 98 (2007) 1528–1535.
[10] J.B. Leppard, Z. Dong, Z.B. Mackey, A.E. Tomkinson, Physical and functional interaction between DNA ligase III alpha and poly(ADP-Ribose) polymerase 1 in DNA single-strand break repair, Mol. Cell. Biol. 23 (2003) 5919–5927.
[11] O. Mortusewicz, J.C. Amé, V. Schreiber, H. Leonhardt, Feedback-regulated poly(ADP-ribosyl)ation by PARP-1 is required for rapid response to DNA damage in living cells, Nucl. Acids Res. 35 (2007) 7665–7675.
[12] H.C. Ha, S.H. Snyder, Poly(ADP-ribose) polymerase is a mediator of necrotic cell death by ATP depletion, Proc. Natl. Acad. Sci. USA 96 (1999) 13978–13982.
[13] Z. Herceg, Z.Q. Wang, Failure of poly(ADP-ribose) polymerase cleavage by caspases leads to induction of necrosis and enhanced apoptosis, Mol. Cell. Biol. 19 (1999) 5124–5133.
[14] P. Pacher, C. Szabo, Role of the peroxynitrite-poly(ADP-ribose) polymerase pathway in human disease, Am. J. Pathol. 173 (2008) 2–13.
[15] S.H. Kaufmann, S. Desnoyers, Y. Ottaviano, N.E. Davidson, G.G. Poirier, Specific proteolytic cleavage of poly(ADP-ribose) polymerase: an early marker of chemotherapy-induced apoptosis, Cancer Res. 53 (1993) 3976–3985.
[16] Y.A. Lazebnik, S.H. Kaufmann, S. Desnoyers, G.G. Poirier, W.C. Earnshaw, Cleavage of poly(ADP-ribose) polymerase by a proteinase with properties like ICE, Nature 371 (1994) 346–347.
[17] D.V. Ferraris, Evolution of poly(ADP-ribose) polymerase-1 (PARP-1) inhibitors, from concept to clinic, J. Med. Chem. 53 (2010) 4561–4584.
[18] Y. Irie, A. Asano, X. Cañas, H. Nikami, S. Aizawa, M. Saito, Immortal brown adipocytes from p53-knockout mice. differentiation and expression of uncoupling proteins, Biochem. Biophys. Res. Commun. 255 (1999) 221–225.
[19] A.M. Dirac, R. Bernards, Reversal of senescence in mouse fibroblasts through lentiviral suppression of p53, J. Biol. Chem. 278 (2003) 11731–11734.
[20] T. Yamanaka, Y. Horikoshi, N. Izumi, A. Suzuki, K. Mizuno, S. Ohno, Lgl mediates apical domain disassembly by suppressing the PAR-3-aPKC-PAR-6 complex to orient apical membrane polarity, J. Cell Sci. 119 (2006) 2107–2118.
[21] T. Tsukada, Y. Tomooka, S. Takai, Y. Ueda, S. Nishikawa, T. Yagi, T. Tokunaga, N. Tokunaga, N. Takeda, Y. Suda, S. Abe, I. Matsuo, Y. Ikawa, S. Aizawa, Enhanced proliferative potential in culture of cells from p53-deficient mice, Oncogene 8 (1993) 3313–3322.
[22] Y. Lu, Z. Nikolovska-Coleska, X. Fang, W. Gao, S. Shangary, S. Qiu, D. Qin, S. Wang, Discovery of a nanomolar inhibitor of the human murine double minute 2 (MDM2)-p53 interaction through an integrated, virtual database screening strategy, J. Med. Chem. 49 (2006) 3759–3762.
[23] S.K. Kumar, E. Hager, C. Pettit, H. Gurulingappa, N.E. Davidson, S.R. Khan, Design, synthesis, and evaluation of novel boronic-chalcone derivatives as antitumor agents, J. Med. Chem. 46 (2003) 2813–2815.
[24] Z. Chen, E. Knutson, S. Wang, L.A. Martinez, T. Albrecht, Stabilization of p53 in human cytomegalovirus-initiated cells is associated with sequestration of HDM2 and decreased p53 ubiquitination, J. Biol. Chem. 282 (2007) 29284–29295.
[25] T. Wang, C.M. Simbulan-Rosenthal, M.E. Smulson, P.B. Chock, D.C. Yang, Polyubiquitylation of PARP-1 through ubiquitin K48 is modulated by activated DNA, NAD+, and dipeptides, J. Cell. Biochem. 104 (2008) 318–328.
[26] C.F. Cheok, A. Dey, D.P. Lane, Cyclin-dependent kinase inhibitors sensitize tumor cells to Nutlin-induced apoptosis: a potent drug combination, Mol. Cancer Res. 5 (2007) 1133–1145.
[27] A.V. Vaseva, N.D. Marchenko, U.M. Moll, The transcription-independent mitochondrial p53 program is a major contributor to Nutlin-induced apoptosis in tumor cells, Cell Cycle 8 (2009) 1711–1719.

The Effect of Resveratrol on the Werner Syndrome RecQ Helicase Gene and Telomerase Activity

Fumiaki Uchiumi[a,*], Takeshi Watanabe[a], Shin Hasegawa[a], Taisuke Hoshi[a], Yoshikazu Higami[b] and Sei-ichi Tanuma[c,d]

[a]*Departments of Gene Regulation,* [b]*Molecular Pathology and Metabolic Disease, and* [c]*Biochemistry, Faculty of Pharmaceutical Sciences, Tokyo University of Science, and* [d]*Genome and Drug Research Center, Tokyo University of Science, 2641 Yamazaki, Noda, Chiba 278-8510, Japan*

Abstract: Various protein factors, including telomerase and WRN helicase, are involved in telomere maintenance. Resveratrol (Rsv), a polyphenol that extends the lifespan of diverse species is an activator of SIRT1, a NAD^+ dependent deacetylating enzyme in mammalian cells. Here, we examined the changes in gene expressions and promoter activities of WRN helicase and telomerase after Rsv treatment. This treatment increased the amount of *WRN* transcript and protein product by activating its promoter and telomerase promoter activity and gene expression. However cell proliferation was not changed. This suggests that Rsv induces telomere maintenance factors like WRN helicase without affecting cell proliferation.

Keywords: BLM, Resveratrol, Telomerase, Sp1, TERT, WRN.

INTRODUCTION

Aging or senescence is a complicated biological process and various factors are involved in its regulatory molecular mechanisms [1-3]. Telomeres, which are the ends of eukaryotic chromosomes, function to protect chromosome ends from fusion and degradation [4]. In human fibroblasts, telomeres are shortened by repeated cell divisions and their length correlates with cellular senescence [4,5]. Progeria syndrome patients are known to show premature aging that is different from normal process. Studies on the human progeroid diseases suggest that nuclear structure and DNA repair systems play important roles in the control of the aging process and life span [6]. Werner's syndrome (WS) patients show also premature aging accompanied with chromosomal instability by mutations on the *WRN* gene, which is involved in DNA repair and telomere maintenance [7]. These observations imply that aging of organisms is controlled by the nuclear functions especially chromosomal maintenance.

Alternatively, aging can be explained by a mitochondrial free radical theory [1]. Reactive oxygen species (ROS) are generated by mitochondrial respiration, and the highly reactive ROS damage inner cellular components including lipids, proteins, and DNA [8]. In some cases, caloric restriction (CR) could reduce ROS production and increases expression of ROS-metabolizing enzymes such as catalase and superoxide dismutases (SODs) [9]. CR extends the mean and maximum life spans of numerous organisms [10]. One of the molecular mechanisms induced by CR is the activation of sirtuins, a conserved family of NAD^+- dependent deacetylases [11]. Resveratrol (Rsv), which is a polyphenol contained in grape skins and red wine, can activate sirtuin-mediated deacetylation [12,13]. Although, it has been reported that Rsv has no obvious effect [14], Rsv could increase median and maximum life spans of yeast, nematode, and fruit flies [12]. In addition, Rsv was reported to improve survival of high-calorie diet mice [15], also suggesting that this compound is a CR mimetic drug. The molecular mechanism of the extension of life span caused by CR is thought to be similar to that caused by Rsv. In order to establish a treatment for aging cells to keep a potency to proliferate and differentiate, it is required to investigate cellular signals induced by Rsv.

In this study, we show that Rsv increases *WRN* promoter activity, and that its gene and protein expressions are accompanied by up-regulation of telomerase in HeLa S3 cells. Moreover, the viability of the cells was not influenced by the treatment for 24 h. These observations suggest that Rsv is an activator of telomerase and WRN without affecting cell death signals.

MATERIALS AND METHODS

Cell Culture

Human cervical carcinoma (HeLa S3) cells were grown in Dulbecco's modified Eagle's (DME) medium (Nacarai, Tokyo, Japan), supplemented with 10% fetal bovine serum (FBS) (Sanko-Pure Chemical, Tokyo, Japan) and penicillin-streptomycin at 37 °C in a humidified atmosphere with 5% CO_2.

Cell Viability Assay (MTS Assay)

An MTS assay was performed as described in the product manual. In brief, cells were cultured in microtiter plate wells with 20 μl of MTS [3-(4,5-dimethylthiazol-2-yl)-5-(3-carboxymethoxyphenyl)-2(4-sulfophenyl)-2H-tetrazolium] solution (Promega, Madison, WI) per well (containing 100 μl

*Address correspondence to this author at the Department of Gene Regulation, Faculty of Pharmaceutical Sciences, Tokyo University of Science, 2641 Yamazaki, Noda, Chiba 278-8510, Japan;
Tel: +81 4 7121 3616; Fax: +81 4 7121 3608;
E-mail: uchiumi@rs.noda.tus.ac.jp

1874-6098/11 $58.00+.00

of cell culture) and incubated for 3 h in a 37 °C, 5% CO_2 humidified incubator. Absorbance at 570 nm was measured by microtiter plate reader (Thermo electron Corp, Vantaa, Finland) and normalized by absorbance at 630 nm.

Construction of Luc-Reporter Plasmids

Luciferase (Luc) reporter plasmids carrying the human *WRN*, *BLM*, *HELB*, *TERT*, and *p21* promoter regions were designated pGL4-BLM, pGL4-HELB, pGL4-WRN, pGL4-TERT, and pGL4-p21 [16]. The Luc reporter plasmid that contains 5'-flanking region of the human Pif1 gene was named pGL4-Pif1 [17].

Transient Transfection and Luc Assays

Plasmid DNAs were transfected into HeLa S3 cells by the DEAE-dextran method [16,18]. After 6 to 24 h of transfection, *trans*-Resveratrol (Cayman Chem., Ann Arbor, MI) was added to the culture medium. After a further 16 to 40 h of incubation, cells were collected and lysed with 100 µl of 1 x Cell culture lysis reagent, mixed, and centrifuged at 12,000 x g for 5 sec. The supernatant was stored at – 80 °C. The Luc assay was performed with a Luciferase assay system (Promega), as described previously [16,18].

Reverse Transcriptase Polymerase Chain Reaction (RT-PCR)

RT-PCR was carried out as described previously [16,18]. First-strand cDNAs were synthesized with ReverTra Ace (Toyobo, Tokyo, Japan), random primers (Takara), and total RNAs extracted from HeLa S3 cells. Primer pairs to amplify human *BLM*, *HELB*, *WRN*, *Sp1*, and *β-actin* cDNAs have been reported previously [16], and the primers for amplifying *SIRT1* cDNAs were hSIRT1-468; 5'- GCGATTGGGTA CCGAGATAAC -3' and hASIRT1-652; 5'- GTTCGAG-GATCTGTGCCAATC -3'. Conditions for the PCR were as follows: 94 °C 30 sec, 55 °C 30 sec, and 72 °C 1 min, with 27 (*BLM*), 26 (*WRN* and *HELB*), 22 (*Sp1*), 22 (*SIRT1*), and 20 (*β -actin*) cycles. PCR products were electrophoresed on 5% acrylamide gels and stained with ethidium bromide.

Quantitative Real-time PCR

Real time PCR analysis was carried out using the Mx3000P Real-Time QPCR System (Stratagene, La Jolla, CA) as described previously [16]. For PCR amplification, cDNAs were amplified using SYBR Green Realtime PCR Master Mix (Toyobo) and 0.3 µM of each primer pair. The primer pairs for amplifying *GAPDH* cDNA were hGAPDH556; 5'- TGCACCACCAACTGCTTAGC-3' and hGAPDH642; 5'- GGCATGGACTGTGGTCATGAG-3'. Amplification was carried out initially for 30 sec at 94 °C, followed by 40 cycles (94 °C 30 sec, 55 °C 30 sec, and 72°C 1 min). Quantitative PCR analysis for each sample was carried out in triplicates. Relative gene expression values were obtained by normalizing C_T (threshold cycle) values of target genes in comparison with C_T values of the *GAPDH* gene using the $\Delta\Delta C_T$ method.

Western Blot Analysis

Western blot analysis was carried out as previously described [16], with antibodies against WRN, and Sp1 (Santa Cruz Biothchnology, Santa Cruz, CA) followed by addition of horseradish peroxidase (HRP)-conjugated secondary antibody (Calbiochem, Darmstadt, Germany). Signal intensities were quantified with an LAS4000 system and MultiGauge Software (Fuji Film, Tokyo, Japan).

Telomerase Amplification Protocol (TRAP) Assay

Cell pellets ($3x10^5$) were treated with 200 µl of ice-cold 1 x CHAPS lysis buffer (10 mM Tris-HCl [pH 7.5], 1 mM $MgCl_2$, 1 mM EGTA, 0.1 mM Benzamidine, 5 mM β-mercaptoethanol, 0.5% CHAPS, and 10% Glycerol), incubated on ice for 30 min, and centrifuged at 12,000 x g for 20 min at 4 °C. The supernatant was then stored at –80 °C. TRAP assays were performed with a TRAP assay kit (Chemicon, Temecula, CA) as described previously [16]. Signal intensities of the DNA ladders and internal controls were quantified with MultiGauge Software.

RESULTS

Proliferation of HeLa S3 Cells After Rsv Treatment

As shown in Fig. (**1**), the proliferation of HeLa S3 cells was not suppressed after 24 h treatment with 40 µM of Rsv measured by MTS. This suggests that Rsv does not induce cell-damaging signals in these experimental conditions.

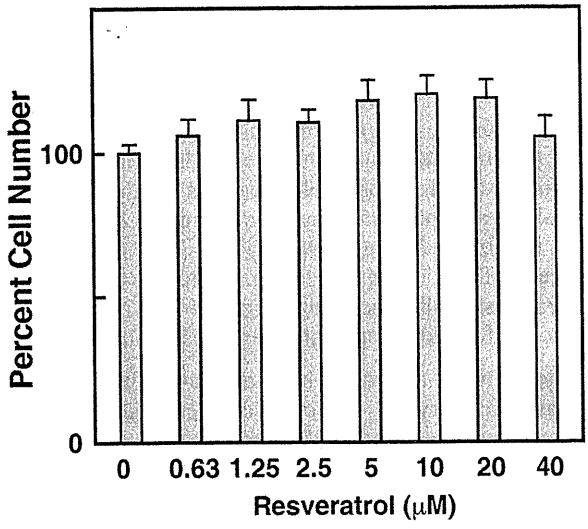

Fig. (1). Resveratrol (Rsv) does not affect proliferation of HeLa S3 cells. HeLa S3 cells were treated with Rsv (1-40 µM) for 24 h. Results represent cell viabilities measured by the MTS assay. The results show the mean ± SD of eight independent experiments.

Augmentation of Expression of DNA Helicase-encoding Genes by Rsv

Quantitative real time PCR showed that the expression of the *WRN*, *HELB*, and *Sp1* genes increased by the increase of the concentrations of Rsv up to 10 µM in the culture medium for 24 h (Fig. **2B**). On the other hand, *BLM* gene expression

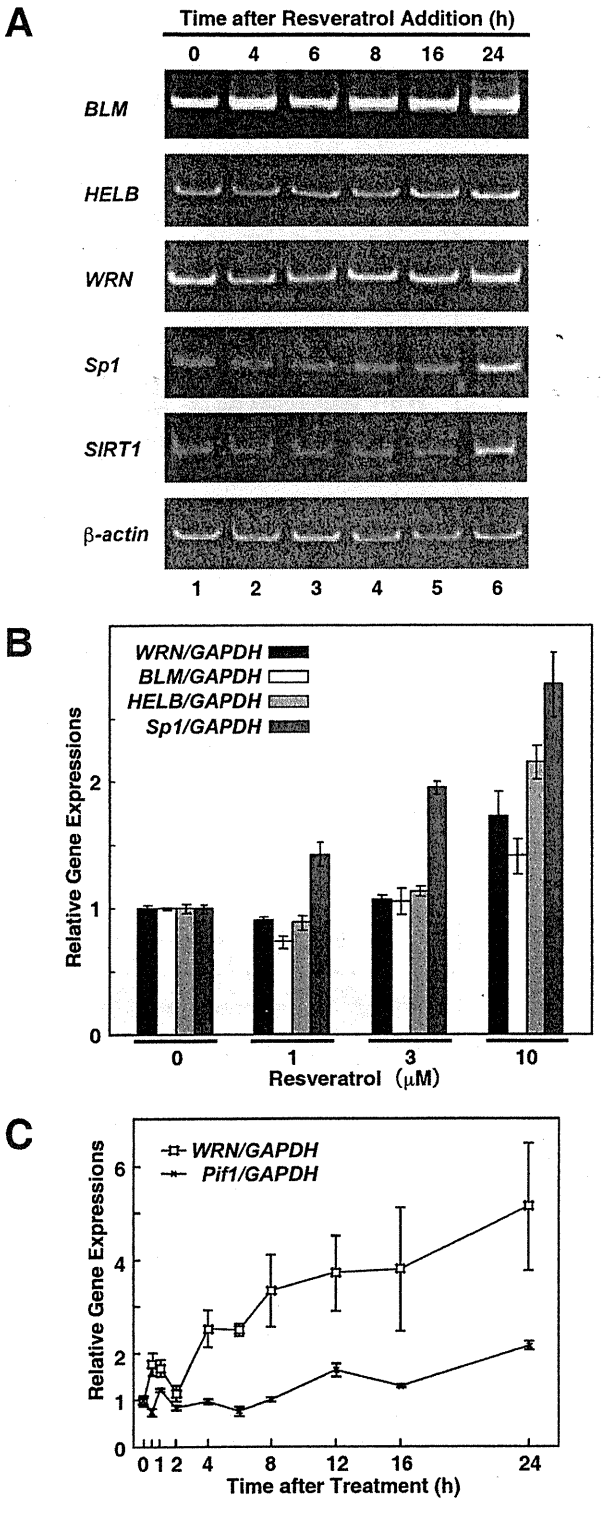

Fig. (2). Changes in gene expressions of various genes after Rsv treatment. (**A**) HeLa S3 cells were treated with 10 μM Rsv for 0, 4, 6, 8, 16, and 24 h (lanes 1, 2, 3, 4, 5 and 6, respectively). Total RNAs were extracted from the cells, and synthesized cDNAs were subjected to PCR with appropriate primer pairs to amplify *BLM*, *HELB*, *WRN*, *Sp1*, *SIRT1*, and *β -actin* cDNA. (**B**) HeLa S3 cells were treated with different concentrations of Rsv (0 to 10 μM) for 24 h. Realtime PCR analyses were performed with cDNA prepared from similar experimental conditions as described above. Results show relative gene expressions of *WRN*, *BLM*, *HELB*, and *Sp1* compared with that of *GAPDH*. The results show the mean ± SD of three independent assays. (**C**) Realtime RT-PCR was carried out to analyze *WRN* and *Pif1* gene expression in HeLa S3 cells after 10 μM of Rsv treatment for 0 to 24 h. The results show relative *WRN/GAPDH*, and *Pif1/GAPDH* gene expression ratios compared with those of Rsv non-treated cells. The values are the mean ± SD of four independent experiments.

was not greatly changed. Next, we examined whether the amounts of *WRN* transcripts were accumulated in a time-dependent manner. As shown in Fig. (**2C**), the relative amount of *WRN* transcripts was greater than those of the *Pif1* transcripts after 4-24 h treatment of 10 μM of Rsv.

Effect of Rsv on the WRN Promoter

To test whether human *WRN*, *BLM*, *TERT*, *p21*, and *HELB* promoters are affected by Rsv treatment, transient transfection experiments were carried out (Fig. **3A**). Luc activities of pGL4-WRN, -BLM, -HELB, -TERT, and -p21 transfected cells were normalized to that of the pGL4-Pif1 transfected cells, because Pif1 has been suggested to have a negative effect on telomere elongation [19]. As shown in Fig. (**3A**), relative Luc activities of these reporter-vector transfected cells were augmented by 10 μM Rsv.

To compare time-dependent responses of the promoters precisely, HeLa S3 cells were treated with Rsv after 6 h of transfection and collected after further incubation from 0 to 40 h. Increases in the *WRN/Pif1* and *TERT/Pif1* promoter activity ratios were observed after 24 h of treatment (Fig. **3B**). Next, Rsv was added after 24 h of transfection, and the cells were harvested after further 0 to 48 h incubation (Fig. **3C**). In these experimental conditions, the magnitude of fold activation of the pGL4-WRN transfected cells after 24 to 48 h Rsv treatment was greater than that of the pGL4-Pif1 transfected cells. Taken together, these results indicate that Rsv up-regulates the *WRN* and *TERT* promoters in HeLa S3 cells.

Expression of WRN Protein After Rsv Treatment

The data above indicate that the *WRN* promoter responds to Rsv and that transcripts are accumulated in the cells. To examine *WRN* protein expression, Western blotting with samples from cells treated with 10 μM Rsv was performed. WRN protein expression increased more than three fold compared with the control level after 16 h Rsv treatment (Fig. **4**). Surprisingly, the amount of WRN protein in 24 h Rsv-treated cells decreased, accompanied by a decrease in Sp1 protein expression (Fig. **4B**). Because *WRN* gene expression increased continuously after 24 h Rsv treatment (Fig. **2**), WRN protein might be down-regulated or degraded at the post-translational level.

Activation of Telomerase by Rsv Treatment

Because similar responses in *WRN* promoter and gene/protein expressions were observed after Rsv, as in the

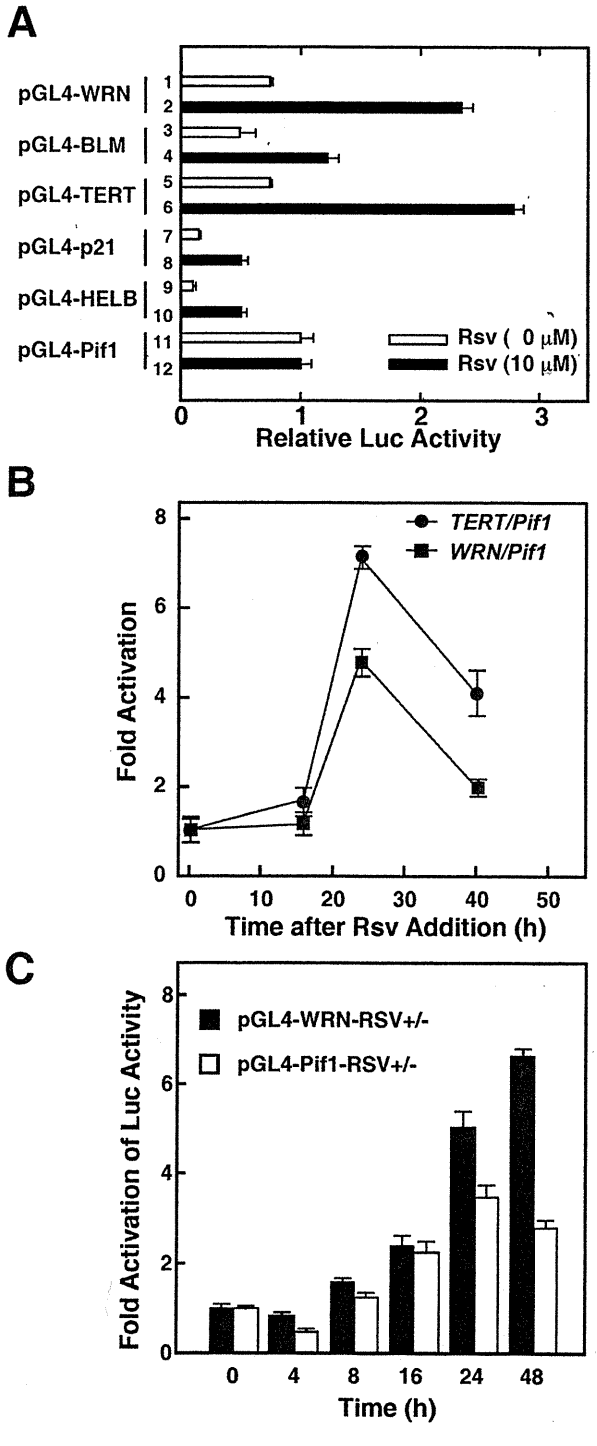

Fig. (3). Effect of Rsv on *WRN*, and *TERT* promoter activities. (**A**) HeLa S3 cells were transiently transfected with pGL4-WRN (columns 1 and 2), pGL4-BLM (columns 3 and 4), pGL4-hTERT (columns 5 and 6), pGL4-p21 (columns 7 and 8), pGL4-HELB (columns 9 and 10), and pGL4-Pif1 (columns 11 and 12). After 6 h incubation, cells were treated with 10 μM Rsv for a further 16 h then Luc samples were prepared. The results show relative Luc activities of these reporter plasmid-transfected cells compared with that of pGL4-Pif1 vector transfected cells. The values are the mean ± SD of four independent assays. (**B**) Similar experiment described in the legend to (**A**) was performed. Fold activation indicates the WRN/Pif1 and TERT/Pif1 promoter activity ratios of Rsv treated cells compared with those of Rsv non-treated cells. The results show the mean ± SD of three independent assays. (**C**) HeLa S3 cells were treated with Rsv after 24 h of transfection. After further 24 h incubation, cells were harvested and Luc assays were performed. The results show relative Luc activities of these reporter plasmid-transfected cells compared with that of Rsv non-treated cells. The values are the mean ± SD of three independent assays.

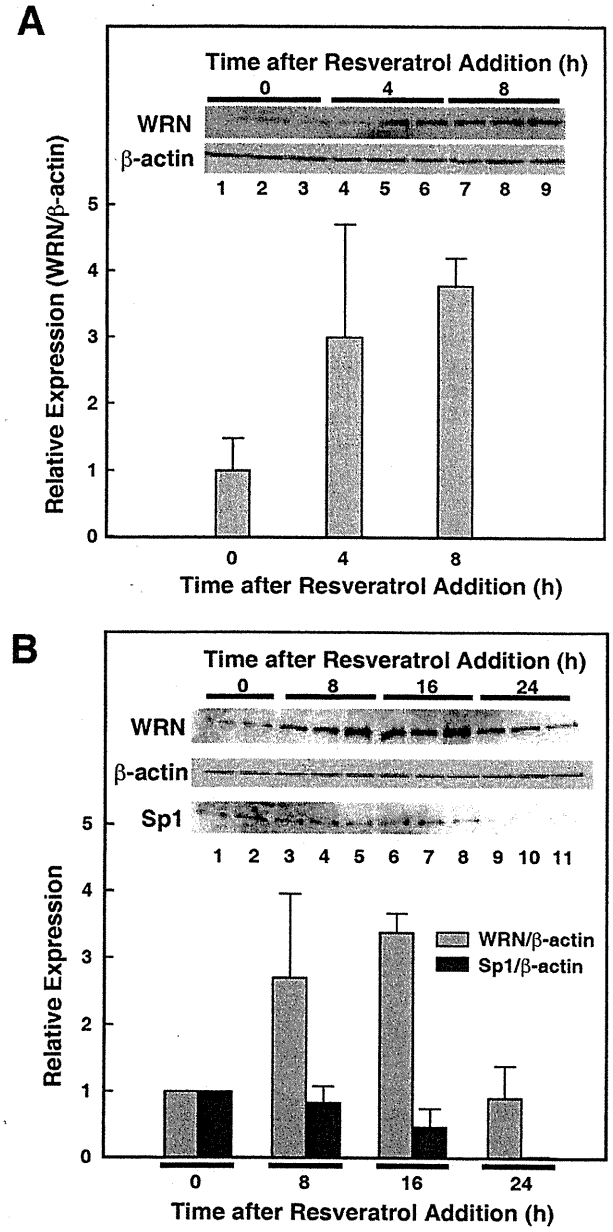

Fig. (4). Rsv treatment-induced amount of WRN in whole protein extracts from HeLa S3 cells. (**A**) HeLa S3 cells (1.0×10^5) were treated with Rsv (10 μM) for 0, 4, and 8 h. Proteins extracted from Rsv-treated cells were separated by a 7.5% SDS-PAGE, and Western blotting was performed with anti-WRN and anti-β-actin antibodies (upper and lower panels, respectively). Then, each band was quantified and results show relative WRN/β-actin protein expression ratio compared to that of the Rsv non-treated cells. (**B**) HeLa

S3 cells were treated with 10 μM Rsv for 0, 8, 16 and 24 h and Western blotting was performed with anti-WRN, anti-β-actin, and anti-Sp1 antibodies. The signal intensity of each band was quantified and the results show relative protein levels compared with that of Rsv-non-treated cells.

case of 2DG treatment [16], we speculated that telomerase might be activated by Rsv. As confirmation, a TRAP assay was performed with the protein samples from HeLa S3 cells treated with 10 μM Rsv for 8 to 24 h (Fig. **5A**). The results showed that telomerase activity reached its highest point at 16 h treatment and decreased after a further 8 h (Fig. **5B**). The pattern of changes of telomerase after Rsv treatment is similar to that of WRN.

DISCUSSION

Genes suggested as controlling the aging process encode proteins involved in DNA-damage responses, DNA-repair synthesis, telomere maintenance, insulin signaling, ROS metabolism, and construction of nuclear membranes [1,3,6]. In other words, the aging process could be affected by alteration of variety of gene expression induced by epigenetic and environmental changes. On the other hand, it seems that the life spans are pre-set or pre-determined by the genome of the organism because the maximum life spans of species are almost constant. From a genetic study of *C. elegans,* it has been suggested that the insulin-mediated signal transduction system plays an important role in controlling life span [20, 21].

CR or reduced caloric intake is the only conclusive and reproducible intervention that can slow aging and maintain health in mammals [22]. Given that insulin enhances cellular glucose intake, CR might have the opposite effect of insulin signaling. Previously, we indicated that 2DG, a potent inhibitor of glucose metabolism, up-regulated the *WRN* gene and protein expressions accompanied by activation of telomerase in HeLa S3 cells [16]. Recent studies have suggested that Rsv also has positive [23] and negative [24] effects on telomerase activity. The effect of Rsv on telomerase might be dependent on whether the experimental conditions induce apoptosis or not. Recently, it was reported that Rsv activates an ATM/ATR-dependent DNA damage response [25]. Therefore, if apoptosis was not induced, Rsv would up-regulate chromosomal DNA maintenance factors including telomerase. In this study, we observed the positive effect of Rsv on *WRN* gene expression and telomerase activity without growth inhibition for 24 h. Rsv is known to be a CR mi-

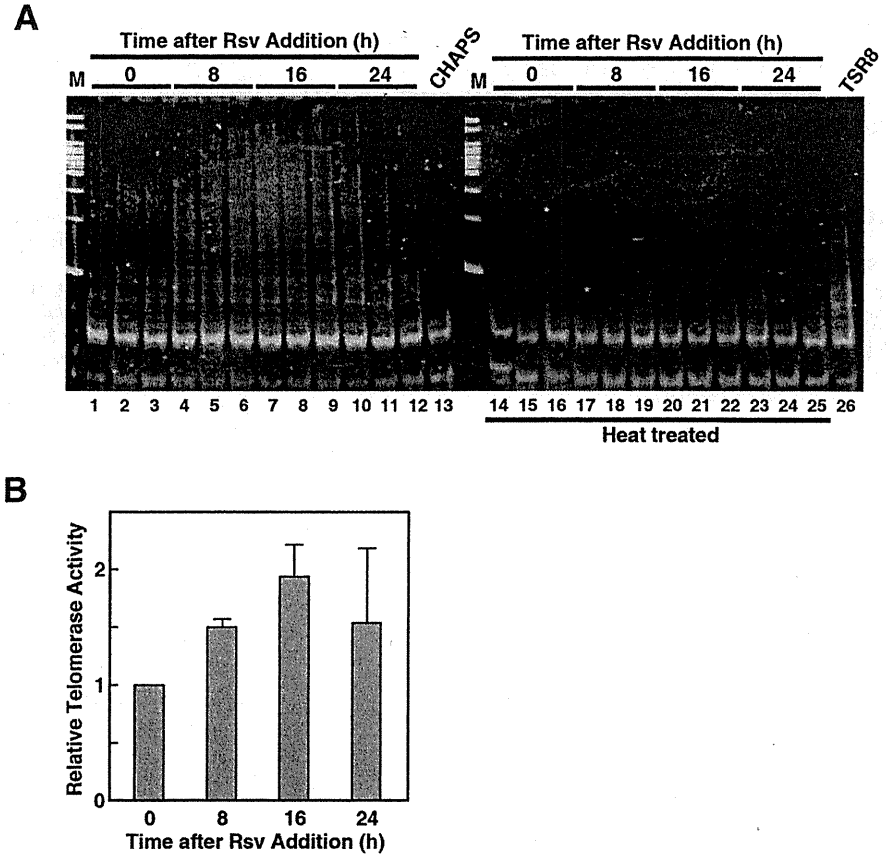

Fig. (5). Rsv treatment induces telomerase activity in HeLa S3 cells. (**A**) CHAPS lysis buffer extracts (20 ng) from HeLa S3 cells were analyzed by the TRAP assay. HeLa S3 cells were treated with 10 μM Rsv for 0 (lanes 1-3), 8 (lanes 4-6), 16 (lanes 7-9), and 24 h (lanes 10-12). Lanes 14 to 25 represent backgrounds with samples that were incubated at 85°C for 10 min. 1 x CHAPS (lane 13) and TSR8 (lanes 26) represent negative and positive controls, respectively. Lane M represents a 100-bp ladder marker. (**B**) Signal intensities of TRAP-products and internal controls were quantified and telomerase activities were calculated as described in the manufacturer's protocol. Histograms show relative telomerase activities compared with Rsv non-treated cells. Results show the mean ± SD of three independent assays.

metic drug that activates sirtuin (SIRT1)-mediated deacetylation [12] and the activation of SIRT1 by Rsv treatment has been reported to improve mitochondrial function [26]. These observations suggest that common signal molecules, such as FoxO [27], might have been affected by 2DG or Rsv to up-regulate promoter activities of the *WRN* and *TERT* genes. In addition, NF-κB activity has been reported to be inhibited by Rsv [28]. Therefore, NF-κB might be one of the candidates for the regulation of the *WRN* and *TERT* promoters. From comparison of the DNA sequence motifs of the *WRN* and *TERT* promoters, multiple GC-boxes or Sp1 binding sequences are commonly found in both promoter regions [16], suggesting that GC-box binding factors are affected by CR mimetic compounds to co-regulate telomere maintenance factors. Because the Sp1 protein decreased after Rsv treatment (Fig. **4B**), other GC-box associating factors might be involved in the positive regulation of the *WRN* and *TERT* promoters. However, these possibilities are yet to be elucidated.

2DG, as a CR mimetic drug, has a very narrow therapeutic range bordering on toxicity, making it difficult to be used as a drug candidate for human beings [22]. On the other hand, Rsv activates SIRT1 but it could induce cell-death or apoptosis [24]. Further analyses are needed to indicate the transcription factor(s) that are responsible for the up-regulation of *WRN* and *TERT* gene expressions by these CR mimetic compounds. Introduction of the expression vectors of these transcription factors with siRNAs for cDNAs of glucose metabolizing enzymes into cells might protect chromosomes and telomeres, thereby elongating life span without toxic effects.

ACKNOWLEDGMENTS

The authors are grateful to Masako Chiba, and Masaya Nomoto for their outstanding technical assistance. This work was supported in part by a Research Fellowship grant from the Genome and Drug Research Center, Tokyo University of Science.

ABBREVIATIONS

BS	=	Bloom's syndrome
CR	=	Caloric restriction
2DG	=	2-deoxy-D-glucose
FCS	=	Fetal calf serum
HELB	=	Helicase B
HGPS	=	Hutchinson-Gilford progeria syndrome
Luc	=	Luciferase
MTS	=	3-(4,5-dimethylthiazol-2-yl)-5-(3-carboxymethoxyphenyl)-2(4-sulfophenyl)-2H-tetrazolium; inner salt
ROS	=	Reactive oxygen species
Rsv	=	Resveratrol
RT-PCR	=	Reverse transcriptase polymerase chain reaction
SDS-PAGE	=	SDS-polyacrylamide gel electrophoresis
SOD	=	Superoxide dismutase
TBS	=	TRIS buffered saline
TRAP	=	Telomerase amplification protocol
WS	=	Werner's syndrome.

REFERENCES

[1] Sanz A and Stefanatos RKA. The mitochondrial free radical theory of aging: A critical view. Curr Aging Sci 2008; 1: 10-21.

[2] Campisi J and d'Adda di Fagagna F. Cellular senescence: when bad things happen to good cells. Nat Rev Mol Cell Biol 2007; 8: 729-40.

[3] Kuningas M, Mooijaart SP, van Heemst D, Zwaan BJ, Slagboom PE and Westerndorp RGJ. Genes encoding longevity: from model organisms to humans. Aging Cell 2008; 7: 270-80.

[4] Blackburn EH. A history of telomere biology. In: de Lange T, Lundblad V, Blackburn E, Eds. Telomeres. 2nd ed. Plainview, NY: Cold Spring Harbor Laboratory Press 2006; pp. 1-19.

[5] Harley CB, Futcher AB and Greider CW. Telomeres shorten during aging of human fibroblasts. Nature 1990; 345: 458-60.

[6] Oberdoerffer P and Sinclair DA. The role of nuclear architecture in genomic instability and aging. Nat Rev Mol Cell Biol 2007; 8: 692-702.

[7] Chu WK and Hickson ID. RecQ helicases: multifunctional genome caretakers. Nat Rev Cancer 2009; 9: 644-54.

[8] Yu BP and Chung HY. Adaptive mechanisms to oxidative stress during aging. Mech Aging Dev 2006; 127: 436-43.

[9] Bokov A, Chaudhuri A and Richardson A. The role of oxidative damage and stress in aging. Mech Aging Dev 2004; 125: 811-26.

[10] Cavallini G, Donati A, Gori Z and Bergamini E. Towards an understanding of the anti-aging mechanism of caloric restriction. Curr Aging Sci 2008; 1: 4-9.

[11] Sinclair DA. Toward a unified theory of caloric restriction and longevity regulation. Mech Ageing Dev 2005; 126: 987-1002.

[12] Stefani M, Markus MA, Lin RCY, Pinese M, Dawes IW and Morris BJ. The effect of resveratrol on a cell model of human aging. Ann NY Acad Sci 2007; 1114: 407-18.

[13] Knutson MD and Leeuwenburgh C. Resveratrol and novel potent activators of SIRT1: effects on aging and age-related diseases. Nutr Rev 2008; 66: 591-6.

[14] Bass TM, Weinkove D, Houthoofd K, *et al.* Effects of resveratrol on lifespan in *Drosophila melanogaster* and *Caenorhabditis elegans*. Mech Aging Dev 2007; 128: 546-52.

[15] Baur JA, Pearson KJ, Price NL, Jamieson HA, Lerin C, Kalra A, *et al.* Resveratrol improves health and survival of mice on a high-calorie diet. Nature 2006; 444: 337-42.

[16] Zhou B, Ikejima T, Watanabe T, Iwakoshi K, Idei Y, Tanuma S, *et al.* The effect of 2-deoxy-D-glucose on Werner syndrome RecQ helicase gene. FEBS Lett 2009; 583: 1331-6.

[17] Uchiumi F, Watanabe T and Tanuma S. Characterization of various promoter regions of human DNA helicase-encoding genes and identification of duplicated *ets* (GGAA) motifs as an essential transcription regulatory element. Exp Cell Res 2010; 316: 1523-34.

[18] Uchiumi F, Sakakibara G, Sato J and Tanuma S. Characterization of the promoter region of the human *PARG* gene and its response to PU.1 during differentiation of HL-60 cells. Genes Cells 2008; 13: 1229-48.

[19] Schulz VP and Zakian VA. The saccharomyces PIF1 DNA helicase inhibits telomere elongation and de novo telomere formation. Cell 1994; 76: 145-155.

[20] Lin K, Dorman JB, Rodan A and Kenyon C. DAF-16: an HNF-3/forkhead family member that can function to double the life-span of *Caenorhabditis elegans*. Science 1997; 278: 1319-22.

[21] Ogg S, Paradis S, Gottlieb S, Patterson GI, Lee L, Tissenbaum HA, *et al.* The Fork head transcription factor DAF-16 transduces insulin-like metabolic and longevity signals in *C. elegans*. Nature 1997; 389: 994-9.

[22] Roth GS, Ingram DK and Lane MA. Caloric restriction in primates and relevance to humans. Ann NY Acad Sci 2001; 928: 305-15.

[23] Xia L, Wang XX, Hu XS, Guo XG, Shang YP, Chen HJ, *et al.* Resveratrol reduces endothelial progenitor cells senescence through augmentation of telomerase activity by Akt-dependent mechanisms. Br J Pharmacol 2008; 155: 387-94.